A REGIONAL STUDY OF PRESSURES, TEMPERATURES, AND AGES OF METAMORPHOSED PELITIC ROCKS IN SOUTHWESTERN MONTANA

Deanna Gerwin

Submitted to the Department of Geology
of Smith College in partial fulfillment
of the requirements for the degree of
Bachelor of Arts with Honors

John B. Brady, Faculty Advisor

May, 2006

Table of Contents

ABSTRACT OF THESIS

A REGIONAL STUDY OF PRESSURES, TEMPERATURES, AND AGES OF METAMORPHOSED PELITIC ROCKS IN SOUTHWESTERN MONTANA

The mountain ranges in southwestern Montana are some of the northwestern-most exposures of Precambrian basement rock of the Wyoming province. The Tobacco Root Mountains are located in this area and have been extensively studied (Brady et. al., 2004) providing new information and questions about the regional geologic history, particularly during the Big Sky Orogeny at 1.77-1.72 Ga. The following is a regional study of metamorphosed pelitic rocks from the Highland, Ruby, and Gravelly Mountain Ranges, which are adjacent to the Tobacco Root Mountains, in order to record the extent and character of Big Sky metamorphism of rocks of similar bulk composition located in different parts of the northern Wyoming Province.

Meta-pelite samples were collected across the region. Thin sections of the meta-pelites were analyzed using a petrographic microscope to identify the minerals present and relevant textures. Using the scanning electron microscope at Smith College, two samples with the assemblage garnet-biotite-quartz-plagioclase-aluminosilicate were analyzed for geothermobarometry using Spear and Kohn's Program Thermobarometry (2001 version). One sample from the Wall Creek area in the Gravelly Mountains and one sample from Camp Creek in the Highlands were sent to the University of Massachusetts for microprobe Th-Pb chemical age dating of monazite grains.

In general, metamorphism seems to be lower grade in the Gravelly Range than in the Highland or Ruby Ranges. For the southern Gravelly Range, a clockwise PT path around the triple point is hypothesized, with andalusite forming first, then kyanite and

finally sillimanite reaching pressures and temperatures of at least 540°C and 3kb (Spear, 1993). A rock from this area gives a date of 2570±45 Ma. The Ruby Range assemblages give a minimum temperature of about 550°C and pressures from about 2.5 to 6.25 kb (Spear, 1993). Results from the Thermobarometry program yield temperatures from about 475-685°C and pressures from about 1.8-5.8 kb. A sample from the Highland Range yields a Th-Pb chemical age of 1819 ± 28 Ma except for two analyses which show a younger average age of 1737± 20 Ma. All samples from the Highland Mountains show evidence of high-grade metamorphism. Many samples contain sillimanite and some show evidence that the reaction muscovite+quartz→ K-spar+ aluminosilicate has occurred. This constrains the temperature to at least 600°C (Spear, 1993). Geothermobarometry has yielded temperatures and pressures that are lower than those expected based on mineral assemblages in both the Highland and Ruby Range samples, possibly due to re-equilibration during cooling.

Two major orogenic events are recorded in the rocks examined for the purposes of this study. The central and southern Gravelly Range show evidence for an older, lower-grade orogenic event (ca 2550 Ma) and do not show clear evidence of the Big Sky orogeny (ca. 1800 Ma). Higher-grade rocks from the Highland and Ruby Ranges to the north, however, give clear evidence of a major orogenic event and high-grade metamorphism at around 1800 Ma. The contrast in character of metamorphism and the difference in ages found in the Gravelly Range show that at least one major structural and/or tectonic boundary runs through the range.

Deanna E. Gerwin
Smith College Department of Geology
Northampton, Massachusetts 01063
May, 2006

ACKNOWLEDGEMENTS

I cannot thank enough my advisor, John B. Brady, for infinite patience, knowledge, advice, ideas, excel graphs, time, dedication to my education, and most of all for believing always in my capabilities even when I didn't. This project could never have even been conceived, let alone realized, without his help. Thank you also to my two field and local advisors, Jack Cheney and Tekla Harms. Both have been a tremendous resource for my project. Thanks to all my Keckies- who have been such a great group of people and whose hard work has helped me with mine. They are all amazing. Thanks to Jack and John also for beautiful field photos, many of which appear as figures in this text.

The entire Smith College Geology Department has been my home at Smith for my three years on campus- the staff and faculty have been incredibly helpful in this project and throughout my Smith College career. Thanks to Tony Caldanaro for being a great boss and for poster-printing and computer advice. To Jon Caris for help with GIS. To Bob Newton, Bob Burger, Mark Brandriss, Amy Rhodes, Al Curran, and Bosijka Glumac, for being a wonderful team of professors and for their genuine concern for the well being of their students. Thanks to Kathy Richardson for cleaning up my messes with the Tomlinson Fund! And for all that she does for our department.

Thanks to all of my fellow Smith geologists for their support, listening to my stupid problems, and for fun in and outside of Sabin-Reed (yay chair races and hiking!!), and especially to Alyssa Doody, my partner in crime and writing companion, without whom I would never have made it through this year. And to my non-geo friends, who reminded me of the outside world and brought me coffee (mostly to Danielle Most, who was a great support to me this year).

Thanks to my family for all their support in my crazy endeavors, especially my grandmothers, Loraine McGowan and Patricia Davidson.

Finally, thanks to the William M. Keck Foundation and the Nancy Kershaw Tomlinson Memorial Fund for financial support.

List of Figures

List of Tables

INTRODUCTION: REGIONAL GEOLOGY AND BACKGROUND

THE WYOMING PROVINCE AND ITS BOUNDARIES

The Precambrian rocks of Southwestern Montana are located in one of seven Archean provinces in the North American craton. These major provinces are the Wyoming, Hearne, Superior, Nain, Slave, Rae, and Burwell. Together they form the protocraton of Laurentia. Three adjacent provinces are important to this study. All samples studied come from one of three different mountain ranges located on the northwestern margin of the Wyoming Province (Fig. 1). The Wyoming province may have formed between 3.2 and 3.4 Ga in a period of crustal growth indicated by dates of detrital zircons (Mueller et al., 1998) and there is evidence indicating that by at least 3.0 Ga "the province existed as a small craton" (Burger, 2004). Except for a small area that represents the southeastern limit of the province, the actual margins of the Wyoming province are not exposed. The southeastern limit is the Cheyenne belt, a shear zone between older (Archean and Early Proterozoic) rocks in the Wyoming Province and Late Proterozoic rocks to the south.

Two other provinces are important to this study because of their relationship to the Wyoming province. The Hearne province lies to the north and the Superior province to the east. Since most of the margins of the Wyoming province are not exposed, it is not well known exactly how and when the three provinces merged. Dates obtained from the Black Hills suggest that the event in which the Wyoming and Superior Provinces collided began ca. 1770 Ma and ended ca. 1715 Ma (Dahl et al., 1999a). The Hearne and Superior provinces collided during the Trans-Hudsonian orogeny, ca. 1860-1790 Ma (Burger, 2004; Dahl et al., 1999a). Dates from the northwestern part of the Wyoming province

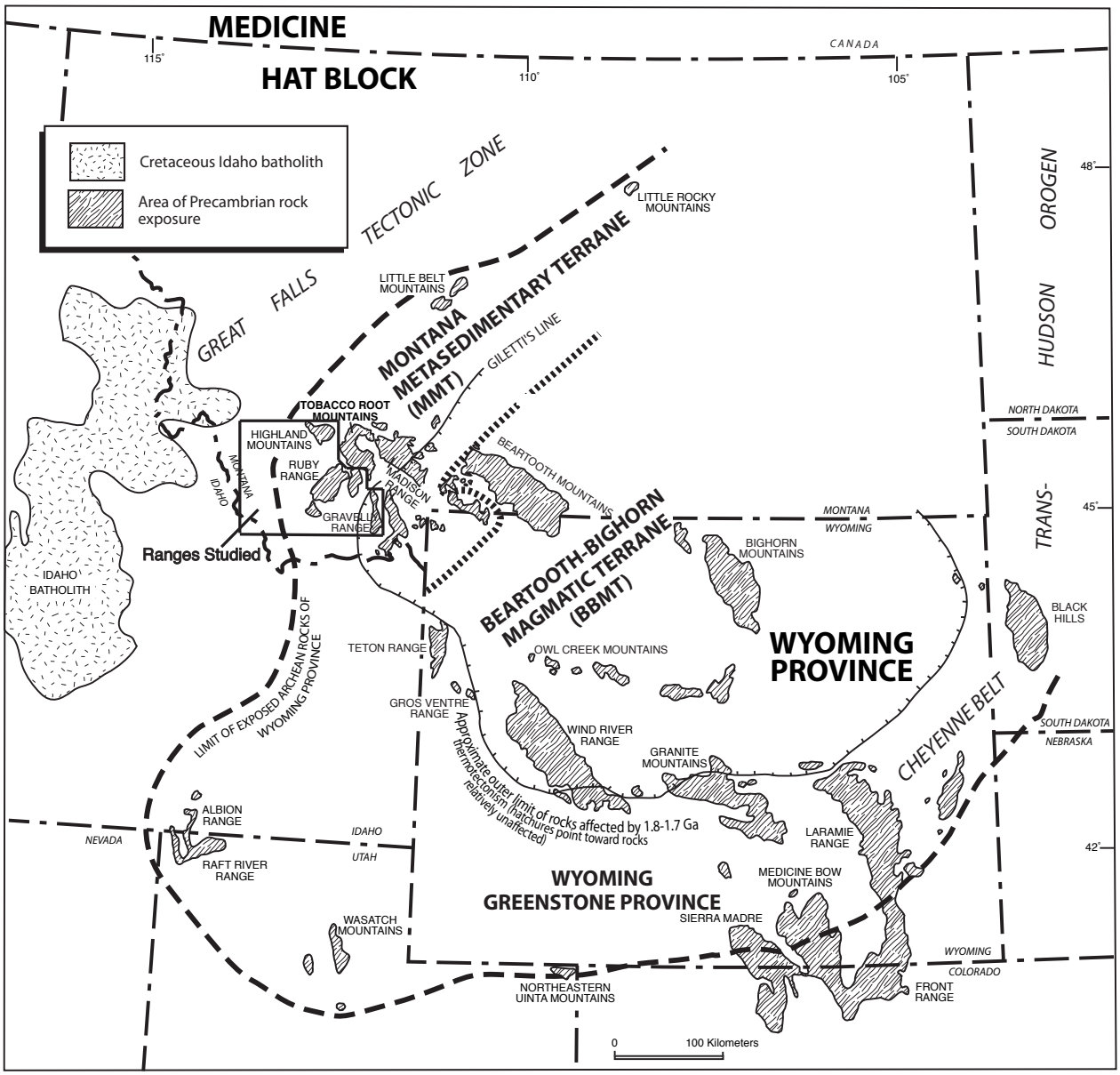

Figure 1: Geology of the Wyoming Province. Ranges studied in this paper (the Highland, Ruby, and Gravelly Ranges) are shown in the boxed area. Modified from Harms et al., 2004.

suggest that the collision with the Hearne Province occurred in the Early Proterozoic (Burger, 2004). The rocks collected for this study come from ranges that are close to the northwestern margin of the Wyoming province and may provide further evidence and information about how the three provinces in question merged.

Various authors have suggested a major Archean-Proterozoic boundary that trends northeast from near Salmon, Idaho and into southwestern Montana based on geochemical and isotopic data (O'Neill 1998). This zone has been extended from the Idaho batholith to just across the Canadian border (Burger, 2004) and is called the Great Falls tectonic zone by O'Neill and Lopez (1985) (refer to Figure 1). It is interpreted to be the possible collisional boundary between the northwestern Hearne province and Wyoming province to the southeast (O'Neill, 1998). This zone shows evidence of recurrent fault movements from "at least the Middle Proterozoic to the Cenozoic, and probably represents a buried zone of crustal weakness" (Burger, 2004). Elements of the Great Falls tectonic zone are similar to other Early Proterozoic orogens in the main part of the Canadian Shield. These tectonic elements can be seen in the Archean rocks of southwestern Montana and include "1) a foreland fold-and-thrust belt that places Archean rocks above" metamorphosed rock that was "likely deposited in an Early Proterozoic foredeep; 2) a 50-mi-wide (80 km), northeast-trending zone of thermally reset K-Ar isotopic systematics in Archean basement rocks…" (Giletti, 1966) "… ; 3) basement involved thrust faults…; and 4) a plutonic-metamorphic zone characterized by amphibolite-grade metamorphism and by mafic to felsic plutons…" (O'Neill, 1998). Despite the similarities noted, some recent electromagnetic data show that the Great Falls

tectonic zone is not like other collision zones in Laurentia and that it may instead be a "reactivated intracontinental shear zone" (Burger, 2004) (see also Boerner et al., 1998).

LITHOLOGIES

Mogk et al. (2004) recognize three distinct rock terranes within the Wyoming province. The Beartooth-Bighorn magmatic terrane contains metaplutonic crystalline rocks: tonalite-trondhjemite-granodiorites dating from ca. 2.7-2.9 Ga (Mogk et al., 1992b). The Wyoming greenstone province is the southernmost terrane, distinguished by greenstone belts with metasedimentary and mafic to ultramafic metavolcanic rocks, the majority of which date between 2.5 and 2.7 Ga (Mueller and D'Arcy, 1990). To the north of the Beartooth-Bighorn subdivision is the Montana metasedimentary terrane. The distinguishing characteristic of this terrane is the presence of metasupracrustal sequences, which contain carbonate-quartzite-pelite groups, "…though quartzofeldspathic gneisses are the dominant lithology" (Burger, 2004) (see also Mogk et al. 1992a, 1992b, 2004). Age dating of the gneisses suggests an igneous protolith of about 3.1 to 3.3 Ga (Burger, 2004; Mueller et al., 1993; Mogk et al., 1992b). The samples in this study came from pelitic units within this terrane.

The relationship of these terranes to one another is not completely clear. All of them have distinctively high $^{207}Pb/^{204}Pb$ for a given $^{206}Pb/^{204}Pb$ ratio, which may indicate similar origin from within the Wyoming province (Mueller et al., 1996). Tectonic relationships, however, are very complex. Zones of faulting and shearing separate the terranes in various locations in the region and "the likelihood of numerous tectonic boundaries suggests caution when attempting correlation from range to range based on

general similarities among lithologies" (Burger, 2004). "Present information suggests that these subprovinces were separate geologic entities that were assembled in the Late Archean, most likely between 2.7 and 2.55 Ga" (Burger, 2004; see also Mogk and Henry, 1988; Mogk et al., 1992b).

The northwestern part of the Montana metasedimentary terrane was known to have experienced a thermal event in the Early Proterozoic based on the work of Giletti (1966). Based on K-Ar age dates determined by Giletti (1966), a boundary called Giletti's line was postulated, separating rocks whose Ar clock had been reset by the 'thermal event' from rocks that seemed unaffected. More recently, evidence has been found that this event was thermotectonic and probably related to the collision of the Hearne and Wyoming provinces. Some dating has been done to show that this event probably occurred somewhere between 1900 and 1700 Ma (Erslev and Sutter, 1990; O'Neill et al., 1988). Structural and petrologic evidence suggest that most of the folds, fabrics and metamorphic minerals are related to a very large-scale orogenic event, called the Big Sky orogeny, rather than a minor thermal event as previously thought, and that it occurred between 1.78 and 1.72 Ga (Burger, 2004).

THE TOBACCO ROOT MOUNTAINS

Most recent research conducted regarding the Early Proterozoic event that affected this area has been done in the Tobacco Root mountains, a range in Southwestern Montana located near the Great Falls tectonic zone (Brady et al., 2004; Tansley et al., 1933; Reid, 1957, 1963; Root, 1965; Burger, 1966, 1969; Hess, 1967; Gillmeister, 1972 ; Cordua, 1973; Hanley, 1975, 1976; Friberg, 1976; Immega and Klein, 1976; Vitaliano et

al., 1979). Early studies had mapped the range, showing major rock units, naming them, and describing lithologies. This information was expanded upon by later studies, and names and groupings of rocks changed as more information was gathered.

A pressure-temperature-time path has been established for the Big Sky orogeny based on studies from the Tobacco Roots. Maximum temperatures and pressures reached up to 1.15 GPa and about 825° C (Cheney et al. 2004).

There are four major suites of rocks described in recent publications on the geology of the Tobacco Roots (Brady et al., 2004). The Indian Creek Metamorphic Suite (some of the rocks in this suite represent part of what were previously called Cherry Creek rocks by some authors (e.g. Gillmeister, 1972)) consists mostly of quartzofeldpathic gneisses but also contains an assemblage of marble, quartzite, pelitic schist and iron formation. A second unit dominated by quartzofeldspathic gneisses is the Pony-Middle Mountain Suite, but it is distinguished from the Indian Creek Metamorphic Suite by the absence of supracrustal rocks and the presence of 'subordinate hornblende gneiss.' The Spuhler Peak Metamorphic Suite (previously called the "Spuhler Peak Formation") is a unit that had previously been grouped with the Cherry Creek rocks but that has since been recognized as a distinct unit by Burger (1966) and Gillmeister (1972). This suite is possibly allochthonous and Proterozoic in age, based on chemical and other differences in composition from the other rock suites. The last group of rocks is the MMDS, metamorphosed mafic dikes and sills. They are found in cross-cutting relationships to gneissic banding and have been found in all suites except the Spuhler Peak formation (Burger, 2004). Whether or not the lithologic packages and information

gathered in the Tobacco Roots can be correlated with the other mountain ranges in the region is not yet clear.

PREVIOUS WORK DONE IN AREA OF STUDY

The Gravelly Range

The Gravelly Range is elongate and runs roughly north-south. Many aspects of the Gravelly Range have been studied (Erslev, 1983, 1988; O'Neill, 1998; Erslev and Sutter, 1990; Vargo, 1990). Lithologies present in the Range are unlike the units present in nearby Ranges in southwest Montana. As O'Neill (1998) observed, "Anomalously low-grade metamorphic rocks, apparently restricted to the southern Gravelly Range are centered on Giletti's line." Although it is still unclear exactly where Giletti's line lies, the northern margin is approximated to run through the northern area of the Gravelly Range (refer to Fig. 1). Another difference noted between the Late Archean rocks in the Gravelly Range and the other assemblages in the region is the lack of carbonate rocks in the southern Gravelly Range (O'Neill, 1998).

Lithologies of the northern Gravelly Range include banded iron formation, sandstone, marble, talc, and phyllites. The phyllites have been determined to contain amphiboles and therefore suggest "an igneous component to the sequence" (Vargo, 1990) (see also Klein, 2006). This is the area I have named after the Luzenac Mine.

Giletti's line has been determined to be located somewhere between Wall Creek and Freezeout Mountain based on K-Ar analyses of micas (Vargo, 1990). This is the central part of the Gravelly Range (Wall Creek in my study).

Further south of the Wall Creek area (Standard Creek area of my study) are sequences of graphitic shale inter-layered with iron formation and intruded by gabbroic sills and plugs. Around the intrusions are contact metamorphic aureoles. Porphyroblasts of andalusite and staurolite have been observed in the aureoles (O'Neill, 1998) (see also Doody, 2006).

The Highland Range

Very little has been written about the Highland Range. The structure of the Highland Mountain Range has been described as an elongate dome (O'Neill et al., 1988) with a gneiss core overlain by quartzofeldspathic gneiss and biotite augen gneiss. Mafic dikes intrude the core and become sills in the overlying, well-foliated gneisses. U-Pb radiometric analysis of zircons (O'Neill et al., 1988) and Ar-Ar ages of biotite (Harlan, 1992) in the overlying gneisses both yield ages of about 1.8 Ga. The mafic intrusions yield a plateau age of 1.79 Ga. Basement rocks exposed in the Highland mountains are some of the "northwesternmost occurrences of cratonic rocks in southwestern Montana" (O'Neill, 1998).

The Ruby Range

The basement rocks of the Ruby Range contain, in apparent stratigraphic order, bottom to top: hornblende and biotite-rich gneiss at the base, quartzofeldspatic and granitic gneiss, a metasedimentary sequence containing dolomitic marble, quartzite, pelitic schist, and aluminous gneiss and schist (O'Neill, 1988) (see also Karasevich et al. 1981; James and Weir, 1972; Vitaliano et al., 1979; Hadley, 1969).

Attempts to determine the relationship between the lithologies in the Ruby Range and Tobacco Root Mountains have shown similarities in both the lithology and structure of the Kelly area of the Ruby Range and the Copper Mountain area of the Tobacco Root Mountains. "The sequence upwards in both areas consists of quartzofeldspathic gneiss, dolomitic marble, amphibolite, quartzite/chert, garnet-biotite-silliminite schist and banded iron-formation. Small tectonically emplaced ultramafic fragments are present in both locales" (Wilson, 1981). These similarities may indicate a similar history and origin of the Ruby Range and the Tobacco Root Mountains.

CHAPTER 1: PURPOSE AND METHODS

STATEMENT OF PURPOSE

The purpose of this study is to determine regional trends of metamorphism in the northwestern Wyoming province and to record the extent and character of Big Sky metamorphism. This was done by collecting samples of similar bulk composition from different mountain ranges in the region. All samples came from the Highland, Ruby and Gravelly Ranges (Figure 2). Because aluminosilicate minerals can be especially useful in determining grade and character of metamorphism, pelitic rocks are ideal for this study.

METHODS OF STUDY

During the summer of 2005, metapelite samples were collected across the region. The presence of aluminosilicate minerals, the amount of weathering, and uniqueness of samples were considered when deciding which samples to collect. For each sample a UTM location was recorded with a GPS unit, outcrops were described and field relationships noted, including strike and dip of foliation if apparent. Most samples were collected from outcrops, but a few float samples were taken if the origin was unambiguous. Twenty-eight thin sections of the metapelites were analyzed using a petrographic microscope to identify the minerals present and interesting textures.

STUDY AREA AND SAMPLE LOCATIONS

Although obtaining a regional distribution of samples was the goal, most samples came from the Highland and Gravelly Ranges, since more Al-rich rocks were found in these areas. Only a few samples came from one location in the Ruby Range. Two areas

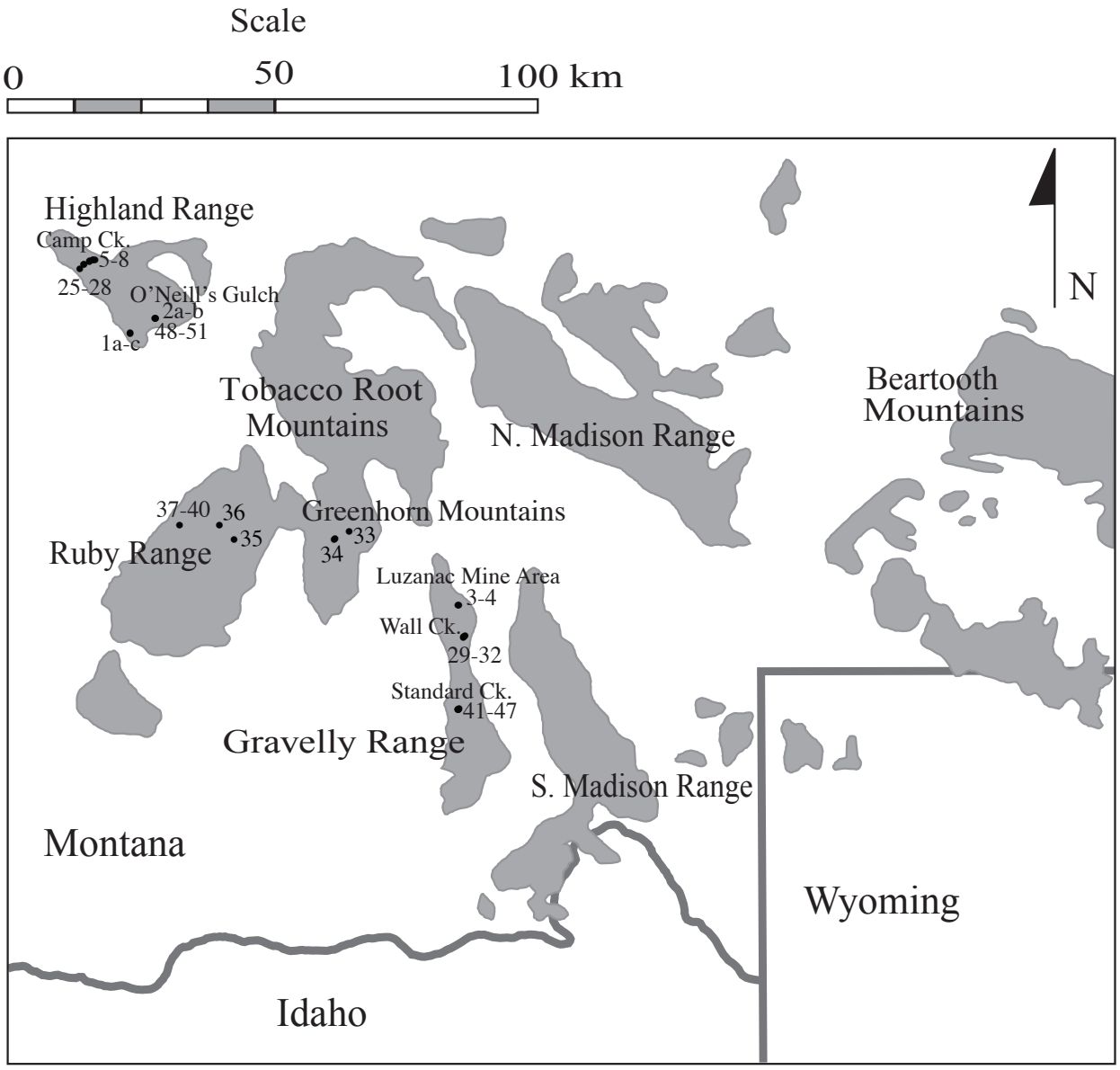

Figure 2: Map of exposures of Precambrian rocks in the northwestern Wyoming province. Sample locations in the Highland, Ruby, and Gravelly Ranges indicated by black dots. Modified from Arthur Schwab, 2006, personal communication.

from the Highland Range were sampled, an area informally called O'Neill's Gulch on the eastern side of the range and Camp Creek on the western side. The Gravelly Range was sampled in three areas, the Luzenac Mine area to the north, Wall Creek in the center, and Standard Creek in the southern region (see Fig. 2 and Table 1 for sample locations).

Table 1: Sample locations and rock types. Locations are given using the NAD 83 datum.

Sample	Easting	Northing	Geographic Location	Rock Type
DG-1a	3845655	5045590	Highlands, O'Neill's Gulch	garnet migmatite
DG-1b	3845655	5045490	Highlands, O'Neill's Gulch	same
DG-1c	3845655	5045490	Highlands, O'Neill's Gulch	same
DG-2a	0389411	5048162	Highlands, O'Neill's Gulch	garnet schist
DG-2b	0389411	5048162	Highlands, O'Neill's Gulch	garnet schist
DG-3a	0443821	5990506	Gravellys, Luzenac Mine Area	fine grained phyllite
DG-3b	0443821	5990506	Gravellys, Luzenac Mine Area	fine grained phyllite
DG-4a	0443970	4990577	Gravellys, Luzenac Mine Area	phyllite, ~10m below gabbro
DG-5a	0378724	5059831	Highlands, Camp Creek	aluminous schist
DG-5b	0378724	5059831	Higlands, Camp Creek	same
DG-6a	0378417	5059892	Higlands, Camp Creek	sillimanite schist
DG-7a	0378255	5059850	Higlands, Camp Creek	float, garnet schist
DG-7b	0378255	5059850	Highlands, Camp Creek	schist
DG-7c	0378255	5059850	Highlands, Camp Creek	garnet, migmatite
DG-8a	0377647	5059687	Higlands, Camp Creek	sill and garnet schist
DG-25	0377593	5059621	Higlands, Camp Creek	sill and garnet schist
DG-26	0376486	5059075	Highlands, Camp Creek	qtzofeld. gneiss with garnet
DG-27	0376428	5059034	Higlands, Camp Creek	garnet migmatite
DG-28	0375700	5058235	Highlands, Camp Creek	aluminous schist
DG-29a	0444465	4984383	S. Gravellys, Wall Ck. Area	phyllite
DG-29b	0444465	4984383	S. Gravellys, Wall Ck. Area	phyllite
DG-31	0444531	4984438	S. Gravellys, Wall Ck. Area	garnet schist
DG-32	0444854	4984719	S. Gravellys, Wall Ck. Area	phyllite w/porphyroblasts
DG-32b	0444854	4984719	S. Gravellys, Wall Ck. Area	phyllite w/porphyroblasts
DG-32c	0444854	4984719	S. Gravellys, Wall Ck. Area	phyllite w/porphyroblasts
DG-33	0423962	5005648	Greenhorns	biotite rich gneiss
DG-34	0421192	5004479	Greenhorns	biotite garnet qtzofeld. gneiss
DG-34b	0421028	5004361	Greenhorns	biotite garnet qtzofeld. gneiss
DG-35	0402116	5005396	Rubies	garnet-bio schist
DG-35b	0402116	5005396	Rubies	garnet-bio schist, float
DG-36	0399487	5008271	Rubies	garnet-bio schist
DG-37	0391889	5008734	Rubies (E side of small gully)	Biotite-orthoamphibole schist
DG-38	~	~	Rubies (W side of same gully)	Garnet-pyroxene metacarbonate
DG-39a	~	~	Rubies (about 10 m W of DG-38)	Sillimanite schist
DG-39b	~	~	Rubies	biotite-sill schist
DG-40	~	~	Rubies (W of sample 39)	garnet-sill schist
DG-41	0442677	4970746	S. Gravellys, Standard Ck.	phyllite, black porphyroblasts
DG-42	0442778	4970893	S. Gravellys, Standard Ck.	graphitic phyllite
DG-43a	0442833	4970861	S. Gravellys, Standard Ck.	garnet schist
DG-43b	0442833	4970861	S. Gravellys, Standard Ck.	garnet schist
DG-44	0442955	4970922	S. Gravellys, Standard Ck.	graphitic phyllite
DG-45	0442958	4970908	S. Gravellys, Standard Ck.	graphitic phyllite
DG-46	0442813	4970872	S. Gravellys, Standard Ck.	garnet phylllite
DG-47	0442669	4970793	S. Gravellys, Standard Ck.	graphitic phyllite
DG-48a	0389391	5048161	Higlands, O'Neill's Gulch	sill and garnet schist
DG-48b	0389391	5048161	Highlands, O'Neill's Gulch	sill and garnet schist
DG-48c	0389408	5048157	Highlands, O'Neill's Gulch	orthoamphibole rock
DG-48d	0389408	5048157	Highlands, O'Neill's Gulch	sillimanite schist
DG-49a	0389522	5048161	Highlands, O'Neill's Gulch	garnet-sill schist
DG-49b	0389522	5048161	Highlands, O'Neill's Gulch	garnet-sill schist
DG-50	0389522	5048161	Highlands, O'Neill's Gulch	biotite-sill schist
DG-51	0389569	5048160	Highlands, O'Neill's Gulch	biotite-sill schist

CHAPTER 2: FIELD OBSERVATIONS

THE GRAVELLY RANGE

Samples were collected from three areas of the Gravelly Range (see Figure 2).

Luzenac Mine Area

The Luzenac Mine Area consists of beds that dip relatively steeply (50-60 degrees) to the northwest, and that generally strike SW-NE. The outcrops observed are metamorphosed sedimentary deposits, which include banded iron formation, quartzite, and phyllite. Cross bedding can still be seen in the quartzite (Fig. 3). The phyllites are all very fine grained, grey to greenish grey in color and exhibit foliation and compositional layering. The bedding planes in the rocks appear flattened. Oxidation weathering is apparent on foliation planes.

The phyllites in the area have been previously studied (Vargo, 1990; Millholland, 1976) and separated into two types based on mineralogy. Type I samples contain biotite, plagioclase and quartz. Type II are phyllites containing chlorite, plagioclase, and quartz, ± biotite, calcite, amphibole and epidote (Vargo, 1990). I have tentatively classified the phyllites collected in this study with the type II phyllites of Millholland (1976) because they are mainly composed of quartz and chlorite. Between two phyllite outcrops a small outcrop that looked like a possible sheared metagabbro was observed. Metagabbro was also observed by Vargo (1990).

Wall Creek

Wall Creek is just south of the Luzenac Mine area. Outcrops of steeply, NW dipping (about 50 to 70 degrees) phyllites can be found on the southeastern side of

Nickerson Creek. Pink colored, garnetiferous quartzofeldspathic gneiss outcrops a few meters to the east. The phyllites strike roughly SW-NE, are dark grey with a bluish cast, and appear knotty or gnarled (Fig. 4). Porphyroblasts can be seen in some samples, and in cross-section may show a chiastolite cross. Other outcrops are lighter colored and lack the porphyroblasts and gnarled appearance. All of the phyllites showed textures indicative of shearing.

Standard Creek

Samples were collected from a phyllite unit about 500 meters from the Standard Creek gabbro intrusion. Banded iron formation surrounds the intrusion, and outcrops seem to grade from iron-rich to more micaceous phyllites. Strike and dip of foliation of most outcrops was difficult to measure, one outcrop (sample DG-45) strikes SE-NW and dips at about sixty degrees to the NE. Outcrops appear very rusty and weathered, breaking easily (especially along planes of foliation). Phyllites are a very dark bluish-grey color and graphitic. Black porphyroblasts are apparent in most outcrops. One outcrop of micaceous garnet schist (DG-43) is greenish-gold in color with garnets about 3 mm in diameter and occurs between units of graphitic phyllite.

Figure 3: Cross bedding visible in quartzite outcrop near the Luzanac Mine. Penny for scale.

Figure 4: Dark bluish-grey phyllite outcrop in Wall Creek. Knotty appearance due to porphyroblasts of alumino-silicate. Penny for scale.

THE RUBY RANGE

Samples come from various places in the Ruby Range, and outcrops were variable in mineralogy. Samples DG-35 and DG-35b came from a biotite-rich outcrop adjacent to an amphibolite on Ruby Reservoir Rd. All other samples came from a hillside gully just off of Stone Creek Road. Units dip 90 degrees and strike roughly NE-SW. Outcrops sampled include sillimanite schist (DG-39b), biotite-amphibole schist (DG-37), biotite-garnet schist (DG-40) and garnet-pyroxene meta-carbonate (DG-38).

THE HIGHLANDS

O'Neill's Gulch

Samples DG-1a, b and c were collected from an area (Nez Perce Gully) about 5.5 km away from the gully that has informally been called O'Neill's Gulch. This outcrop shows signs of partial melting. The leucosome parts of the outcrop are rich in feldspar, quartz and garnet while the restite is more biotite-rich and schistose. Strike of foliation planes of the outcrop was SE-NW with a moderate dip of about forty-two degrees to the SW.

All other samples (ten in total) come from O'Neill's Gulch. The strike and dip of one outcrop is 052/75SE (samples DG-2a and b come from this outcrop) and in the field units appear to be relatively similar in orientation. Some outcrops in this area seem very deformed or possibly sheared and have a broken appearance (Fig.5). A few pelitic outcrops are adjacent to amphibolites. Some outcrops show compositional layering with lens-shaped felsic bodies that could be due to partial melting.

Figure 5: Deformed sillimanite schist beds in O'Neill's Gulch. Hammer (about 2.5 feet long) for scale.

Camp Creek

Ten samples were collected from this area. Outcrops are mostly gneisses, some with pelitic layers. Compositional layering can be observed in some outcrops, alternating quartz-rich layers with pelitic layers. Strong foliation can be observed and sillimanite is commonly lineated along foliation planes, varying from .5-1 cm in length. Strikes and dips of the outcrops vary. The eastern-most outcrops (samples DG-5a and b, 6a) strike roughly NW-SE and dip about 20 degrees NE. Outcrops downstream (further west) strike roughly NE-SW and maintain a shallow dip of 15-30 degrees SW. Compositional differences within the outcrops seem to indicate partial melting (felsic bodies seem to 'float' in darker restite). Garnets appear dark and altered in hand sample.

CHAPTER 3: PETROGRAPHY AND SAMPLE DESCRIPTIONS

THE GRAVELLY RANGE

The Luzenac Mine Area

This is the northernmost area sampled in the Gravelly Range. Outcrops sampled from this area are very fine-grained, chlorite-rich phyllites. Most of the rocks do not seem severely deformed, but some folds in quartz layers occur. Only one sample (DEG-3b) (just south of the Luzenac mine) was made into a thin section, a very fine-grained, lightly foliated phyllite that is grey-green in color. Some oxidation has occurred, especially along planes of foliation. Compositional layering is visible in thin section at a high angle to foliation and appears to be original depositional bedding planes in the rock, alternating quartz-rich layers with very fine-grained mica minerals (Fig. 6). The thin section was too fine-grained for significant optical identification of minerals other than quartz. XRD analyses show peaks congruent with chlorite and quartz (see appendix) and, judging from the thin section, these minerals compose at least 95% of the rock. Lineation of grains is parallel to foliation planes. Quartz grains are larger than other mineral grains.

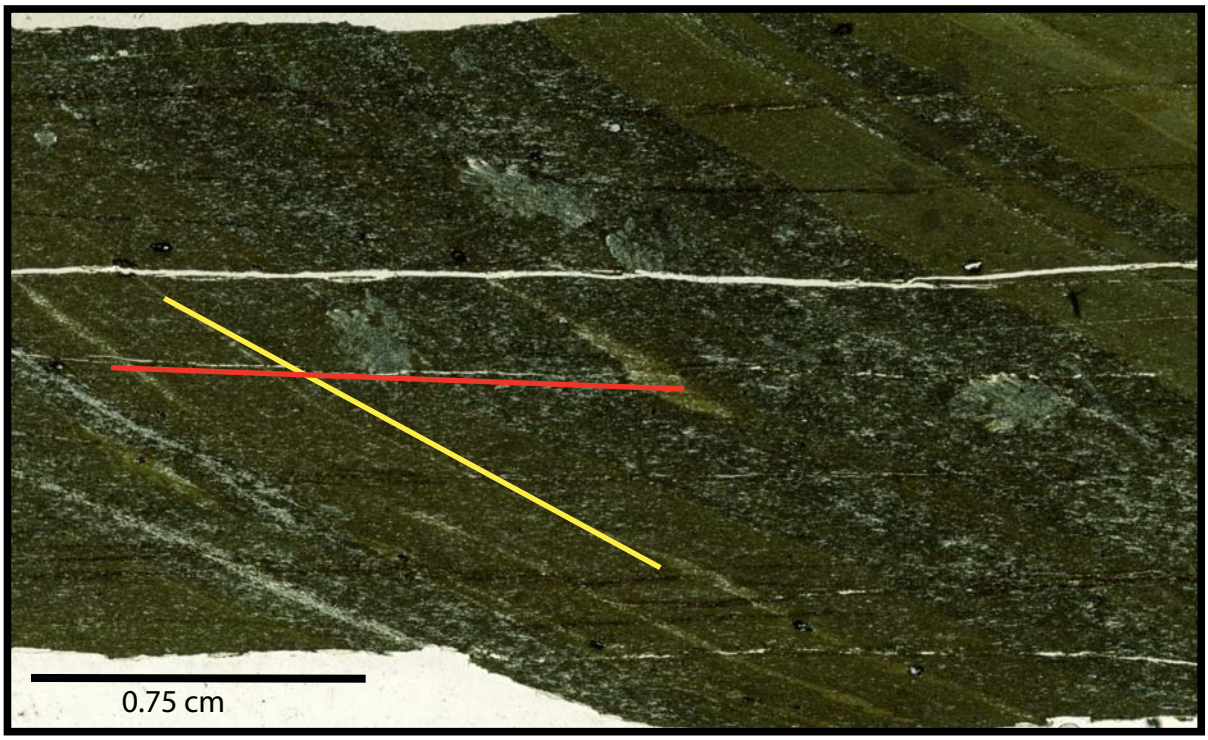

Figure 6: View of thin section of sample DG-3b from the Luzanac Mine area. Depositional bedding can be seen at an angle to foliation. Yellow line shows orientation of depositional bedding, red shows orientation of foliation planes.

Wall Creek

The Wall Creek area of the central Gravelly Range consists of outcrops of dark bluish-grey, fine-grained rock, some with porphyroblasts of aluminosilicate containing a chiastolite cross (Fig. 7a). Of six samples collected, four samples were analyzed in thin section. Most samples contain staurolite, biotite, quartz and aluminosilicate. One sample of different bulk composition (DG-30) contains garnet, biotite, quartz and a green amphibole. Many samples show shearing textures and cryptic overgrowth of minerals.

Although the porphyroblasts present in some outcrops were thought to be andalusite, it is clear in thin section (sample DG-32a) that they are actually bundles of prismatic kyanite pseudomorphed after andalusite (Fig. 7b).

One sample of fine-grained phyllite, DG-29, contains both prismatic kyanite and fibrous sillimanite. Commonly the fibrolite grows around the kyanite in such a way as to suggest that it came after the kyanite. There are other fragments of a moderately high relief alumino-silicate mineral that has inclusions in the center of vertical sections of the grains. All of these minerals occur in close proximity in the thin section (Fig.8). Other significant minerals in this sample include staurolite, biotite, and muscovite. It is also important to note that the rock shows shearing textures.

Figure 7a: Cross-section view of alumnosilicate porphyroblast in sample DG-32a from Wall Creek. In thin section it is clear that the porphyroblast is prismatic kyanite pseudomorphed after andalusite (note chiastolite cross). Penny for scale.

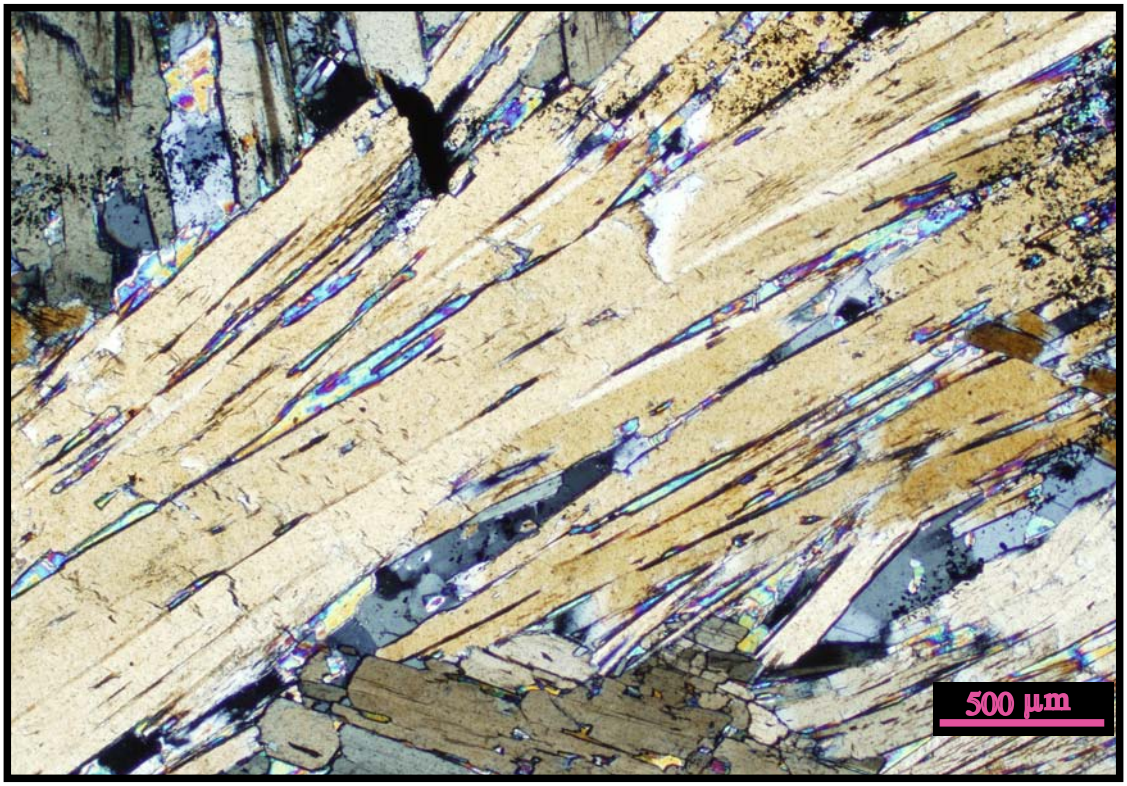

Figure 7b: Thin section view of bladed kyanite from sample DG-32a under cross polarized light. The chiastolite trail of inclusions can be seen at the top of the view.

Wall Creek	Mineralogy	Textures/Notes
DG-29	Quartz, biotite, plagioclase, muscovite, kyanite, staurolite, sillimanite (fibrous), opaque mineral	All minerals broken and angular, shearing textures
DG-30	Garnet, quartz, amphibole, biotite, plagioclase	Alteration of plag to sericite, alternating amphibole/felsic rich compositional layering, strong lineation of minerals
DG-32a	Staurolite, biotite, plagioclase, graphite, opaque mineral, quartz, kyanite	Graphite inclusions, some staurolite overgrowing previous textures, porphryoblast (1.4 cm) of alumino-silicate-kyanite pseudomorphed after andalusite
DG-32b	Staurolite, quartz, biotite, plagioclase kyanite, sillimanite (fibrous), graphite	Fractured grains, sheared texture.

Table 2: Mineralogy and textures observed in thin sections from Wall Creek.

Standard Creek

Eight samples were collected from various locations about 460 meters from the Standard Creek contact aureole and six were made into thin section. All the rocks collected from the Standard Creek area are dark grey phyllites except the two DG-43 samples, which are from an outcrop of garnet schist. Rocks from this area are highly weathered, showing iron oxidation (especially on foliation planes) and are easily broken. The grey color of the phyllites is due to abundant graphite, with is concentrated as inclusions within porphyroblasts of a mineral, causing the rock to appear to have porphyroblasts of a black mineral (Fig. 9a). Analysis of the porphyroblasts in sample DG-44 with the scanning electron microscope (SEM) showed that they are in fact albite. The SEM showed that some potassium was present as well, probably due to overgrowth of muscovite, which can be seen in thin section (Fig. 9b). In some rocks the graphite inclusions are concentrated in crystals of staurolite, which exhibit zoning with rims that

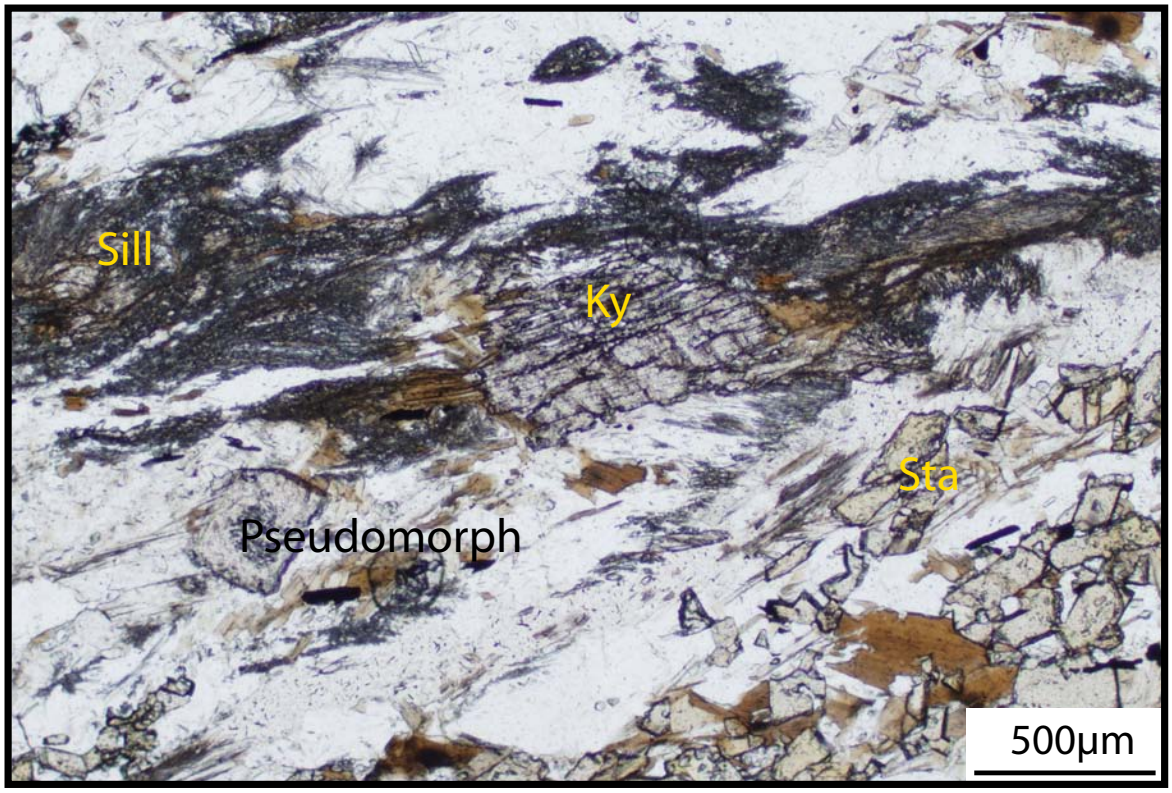

Figure 8: Thin section of sample DG-29 from Wall Creek in plane light. Fibrous sillimanite (sill), prismatic kyanite (ky), stuarolite (sta), and a possible pseudomorph are visible.

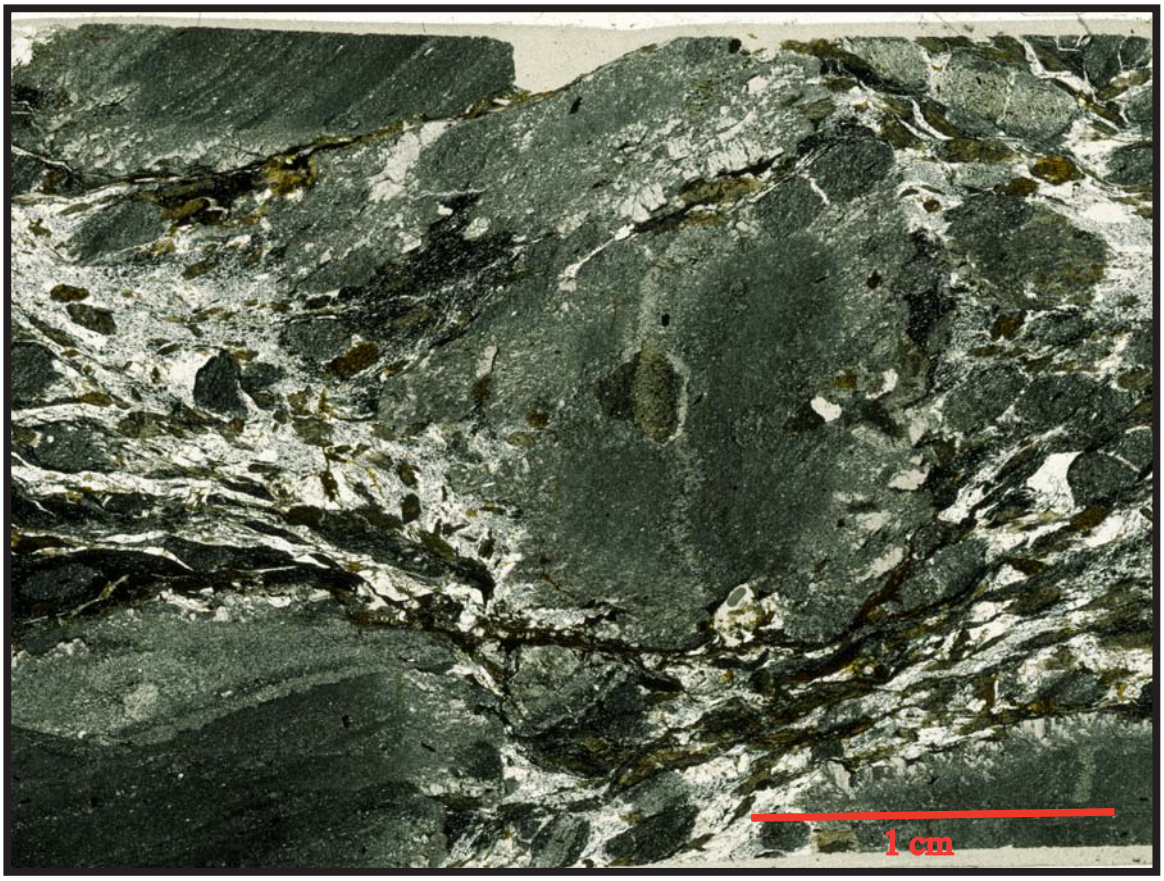

Figure 9a: Black porphyroblasts in sample DG-45 from Standard Creek. Scan of entire thin section (plane light).

have less graphite (Fig. 10). The porphyroblasts vary in size from .2-3 cm, some outcrops with larger ones and some with smaller ones. Garnets in samples DG-43a and b range from .2-.4 cm in diameter. The rest of the rock is greenish in color, micaceous, and rusty along foliation planes.

Standard Creek	**Mineralogy**	**Textures/Notes**
DG-41	Graphite, quartz, muscovite, chlorite (retrograde?), plagioclase, andalusite	Chlorite overgrowing other minerals, porphyroblasts with graphite inclusions, wavy appearance.
DG-42	Andalusite, quartz, graphite, muscovite, chlorite (retrograde?)	Minerals overgrow each other (esp. chlorite), wavy fabric, andalusite pophryoblast about 2 cm in diameter.
DG-43a	Chlorite, abundant opaque mineral, garnet, quartz	Garnets with abundant quartz inclusions
DG-44	Sillimanite (fibrous), graphite, muscovite, biotite, chlorite, quartz	Muscovite and chlorite overgrow graphitic porphyroblasts.
DG-45	Biotite, muscovite, quartz, graphite, staurolite	Porphyroblasts with graphite.
DG-46	Staurolite, garnet, plagioclase, biotite, muscovite, quartz	Graphite inclusions in staurolite, though sometimes less in the rims.

Table 3: Mineralogy and textures observed in samples from Standard Creek.

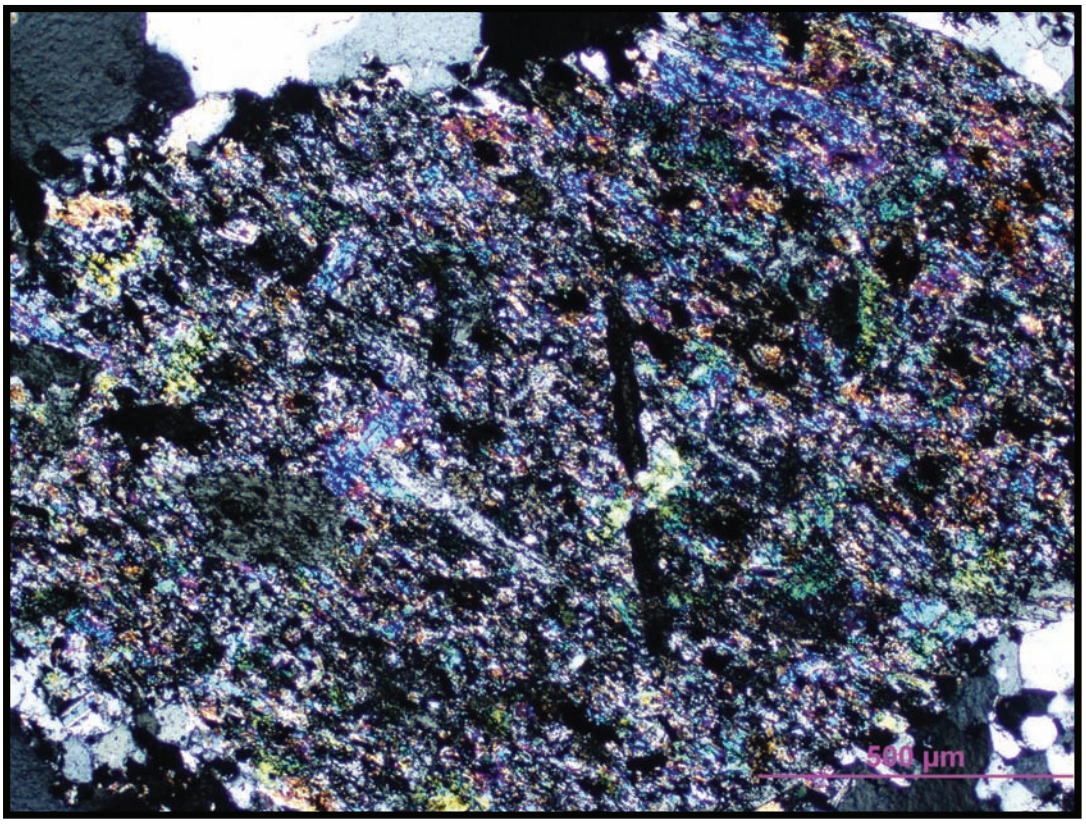

Figure 9b: Photomicrograph of porphyroblast in sample DG-44 from Standard Creek. Cross polarized light. The porphyroblast is plagioclase with abundant graphite inclusions, overgrown with muscovite and chlorite.

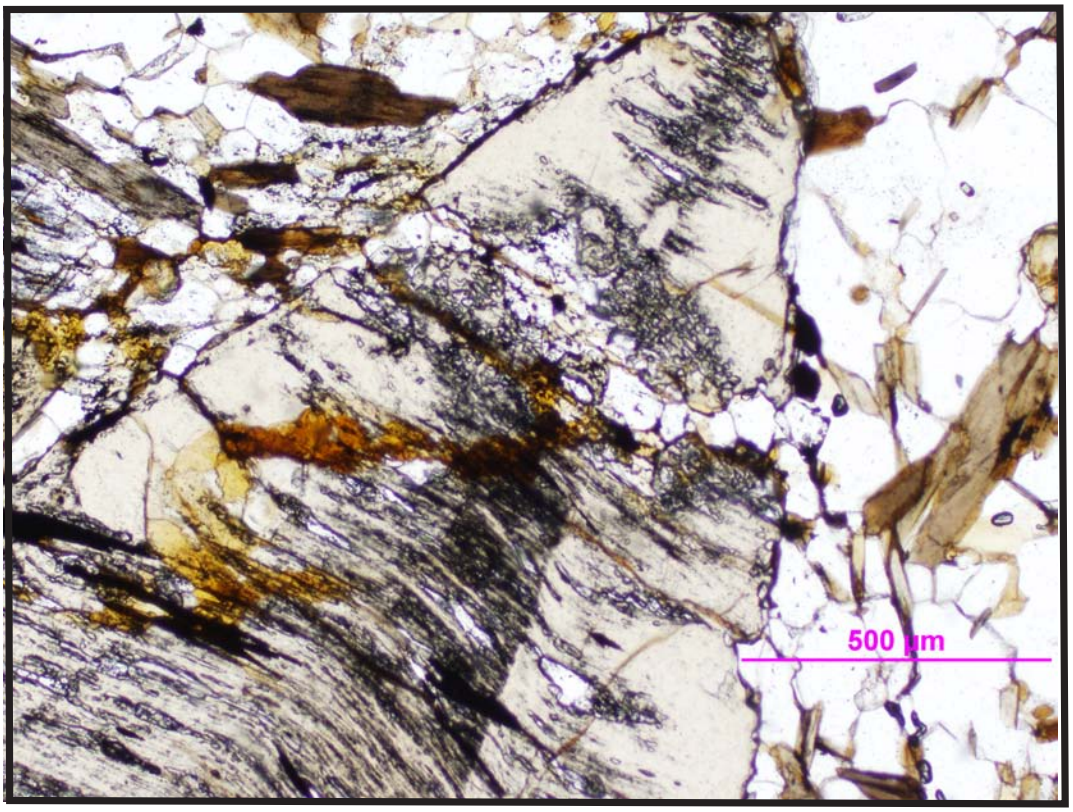

Figure 10: Photomicrograph of zoned stuarolite with inclusion free rim from sample DG-46, Standard Creek. Plane light.

THE RUBY RANGE

Of eight samples collected from the Ruby Range, five were made into thin sections. Samples from this area varied from biotite-rich amphibolite to aluminous schist. All samples contained minerals reflecting high-grade metamorphic conditions. Aluminous rocks contained sillimanite, biotite, plagioclase and quartz ± muscovite ± garnet. Most sillimanite in these samples occurs as fibrous aggregates. In one sample, DG-39b, lens-shaped, mat-like aggregates 2-3 cm long and .25-.5cm wide are visible in hand sample and in thin section (Fig. 11). Elongate minerals are aligned parallel to foliation (if present).

Ruby Range	**Mineralogy**	**Textures/Notes**
DG-35b	Plagioclase, biotite, quartz, garnet, sillimanite, rutile monazite	Fine-grained (<1mm), some garnet altering to sericite
DG-37	Quartz, biotite, garnet, plagioclase, kyanite(?) with staurolite in pockets, orthoamphibole	Elongate grains (1-2mm long) of orthoamphibole, lineation parallel to foliation
DG-38	Zoned tourmaline, calcite, quartz, garnet, biotite, diopside(?)	Fine-grained matrix with larger garnets
DG-39b	Biotite, sillimanite (fibrous), feldspar, quartz, muscovite	Sillimanite occurs as fibrous mats (up to 3 cm long and .5 cm wide)
DG-40	Biotite, quartz, sillimanite (fibrous), garnet	Garnets poikiloblastic, anhedral and intergrown with other minerals in matrix

Table 4: Mineralogy and textures observed in thin sections from the Ruby Range.

THE HIGHLAND MOUNTAINS

O'Neill's Gulch

Of the thirteen samples collected at O'Neill's Gulch, six thin sections were made. Sample DG-1 a,b and c were collected from Nez Perce (about 5.5 km away from

O'Neill's Gulch, see Chapter 2). Like Camp Creek, the dominant mineral assemblage in samples from O'Neill's Gulch is sillimanite-garnet-biotite. Muscovite, plagioclase, and quartz are also found in most samples. One sample, DG-50, is different than the others. It does not contain garnet, but does contain corundum and microcline. More pelitic layers containing biotite, sillimanite and muscovite surround lens-shaped felsic bodies. Garnets in all samples commonly have a poikiloblastic texture, with quartz and biotite inclusions. In many samples it appears that the rims of the garnets have fewer inclusions than the cores (Fig. 12). Garnets from O'Neill's Gulch do not seem as fractured as those in rocks from Camp Creek. Most of the sillimanite occurs as fibrolite, unlike rocks in Camp Creek, although some samples show prismatic sillimanite as well. Elongate minerals in samples from this area commonly show lineation parallel to foliation planes.

O'Neill's Gulch	**Mineralogy**	**Textures/Notes**
DG-1b (Nez Perce)	Biotite, chlorite (retrograde?), garnet, plagioclase, quartz, muscovite, monazite, rutile	Garnets poilkiloblastic, some with sericite alteration around edges and biotite and chlorite growing in fractures
DG-2a	Sillimanite (prismatic), garnet, biotite, quartz, plagioclase, rutile, illmenite	Poikiloblastic garnets with quartz and biotite inclusions. Rims are often inclusion free. Some sericite alteration around sillimanite.
DG-48a	Sillimanite, garnet, quartz, biotite, plagioclase	Sillimanite (fibrous and prismatic) alters to sericite.
DG-48b	Garnet, quartz, biotite, plagioclase, sillimanite, rutile	Garnet inclusions (mostly quartz) but not as much in rims
DG-49a	Sillimanite, biotite, quartz, garnet, plagioclase	Garnet porphyroblasts (1-2cm) showing fabric at an angle to lineation of elongate minerals, fibrous and prismatic sill.
DG-50	Biotite, plagioclase, muscovite, sillimanite, microcline, quartz, corundum	Lens shaped felsic bodies contain microcline, darker, more fine grained minerals in surrounding rock.

Table 5: Thin section mineralogy and textures from O'Neill's Gulch, Highland Range.

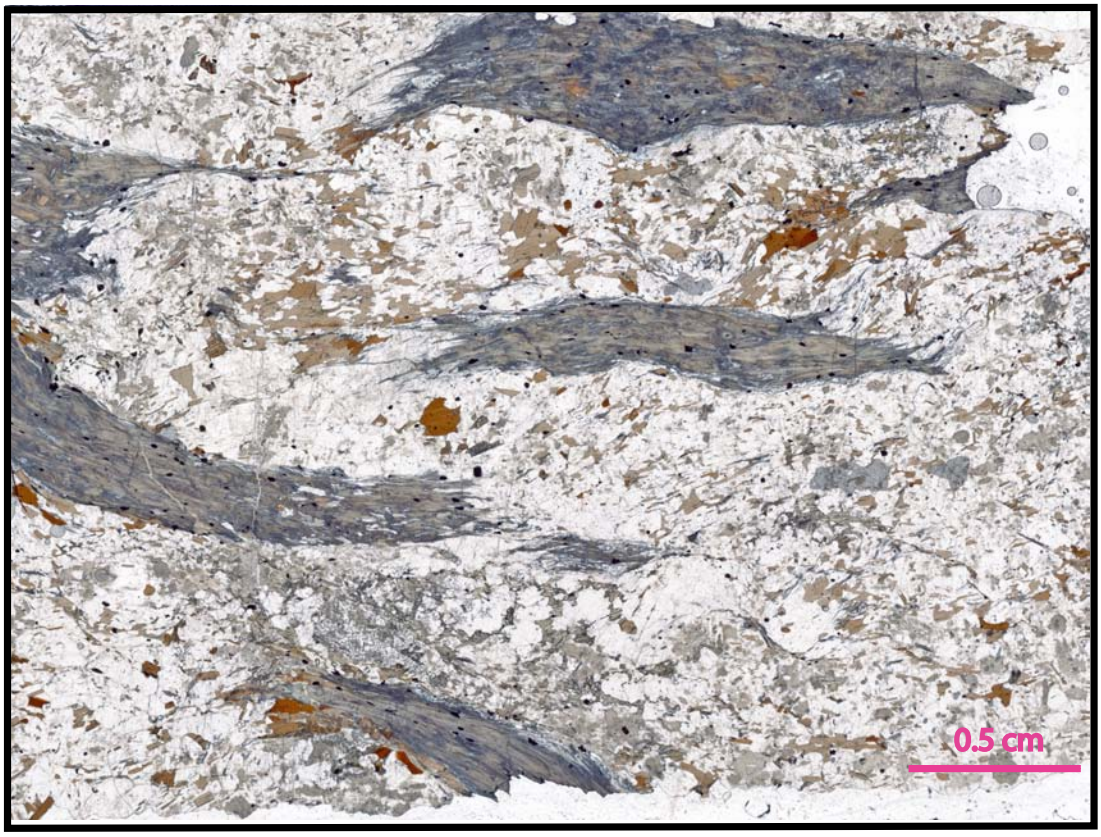

Figure 11: Sillimanite mats viewed in a scan of entire thin section from the Ruby Range (DG-39b). Here the color is a little off, they are actually more beige colored. (Plane light).

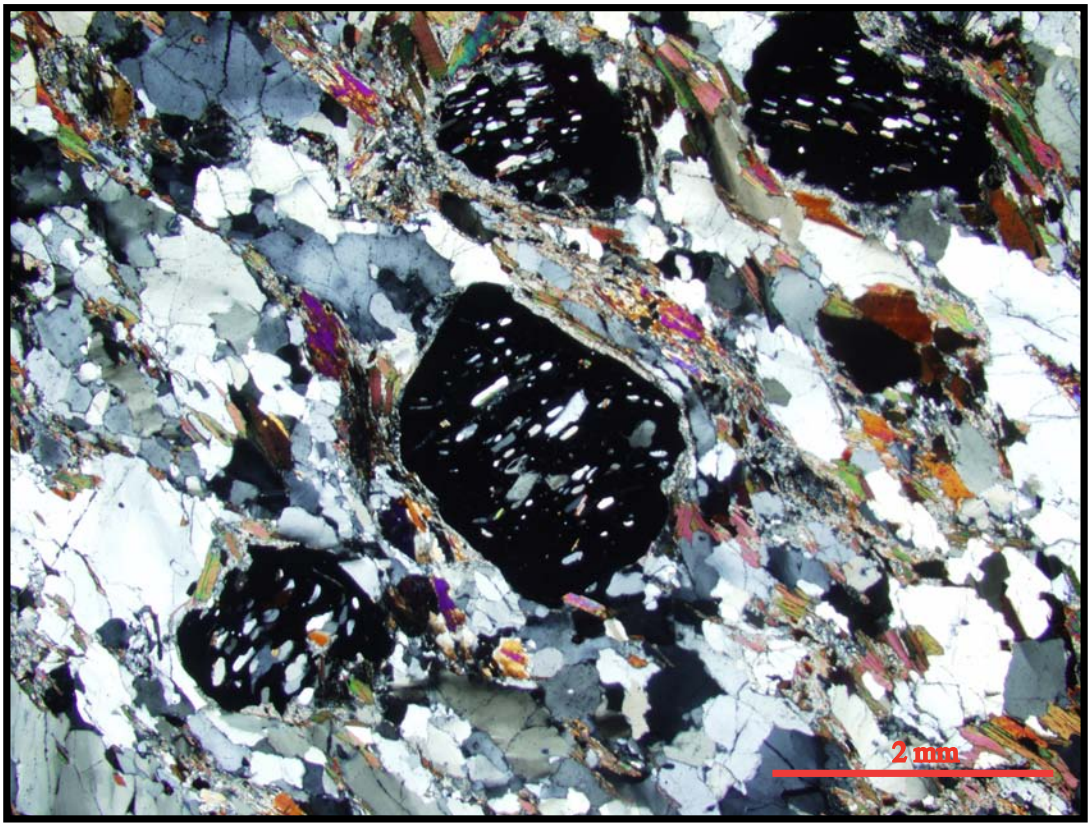

Figure 12: Garnets in thin section from O'Neill's Gulch (DG-2a). Crossed polars. Some garnets (center) have inclusion free rims. Also visible are quartz, biotite, and sillimanite.

Camp Creek

Eleven samples were collected from the Camp Creek area in the northwestern part of the Highland Range. Of these, five were examined in thin section (Table 6). Most thin sections contained sillimanite (prismatic only), biotite and garnet. Other minerals commonly observed in thin section include muscovite, quartz, plagioclase and microcline. In one sample, DG-6a, microcline and sillimanite occur in the absence of muscovite. Sericite occurs as an alteration around sillimanite and garnet in many samples, and feldspar is commonly altered by hydration. Migmatitic textures can be observed in the field and in thin section, suggesting that the rocks had begun to melt during metamorphism. Garnets are commonly fractured and show a poikiloblastic texture, with biotite and sillimanite growing inside the fractures and quartz, feldspar or biotite inclusions within the garnet (Fig. 13). Some samples have a wavy appearance and lens shaped felsic bodies, perhaps due to partial melting of the rock (Fig. 14).

Camp Creek	**Mineralogy**	**Textures/Notes**
DG-5a	Sillimanite (prismatic), garnet, muscovite, biotite, quartz, plagioclase	Garnets are very fractured, with biotite often growing in the fractures. Sillimanite alters to sericite.
DG-6a	Garnet, biotite, microcline, plagioclase, quartz, sillimanite, opaque mineral	Garnets very fractured, biotite grows in fractures, hydration of feldspar, sericite alteration of garnet, sillimanite. Lensoid felsic bodies (Fig. 5).
DG-7b	Biotite, muscovite, quartz, garnet, sillimanite	Sericite alteration throughout rock, lensoid wavy texture
DG-8a	Biotite, chlorite (alteration of biotite), garnet, quartz, muscovite, plagioclase, sillimanite	Very fractured garnets with biotite and sillimanite growing in fractures, sericite alteration throughout rock.
DG-28	Muscovite, biotite, quartz, plagioclase, microcline, garnet, rutile	Alternating layers of more biotite rich and more felsic minerals (including microcline)

Table 6: Minerals and textures observed in thin sections from Camp Creek.

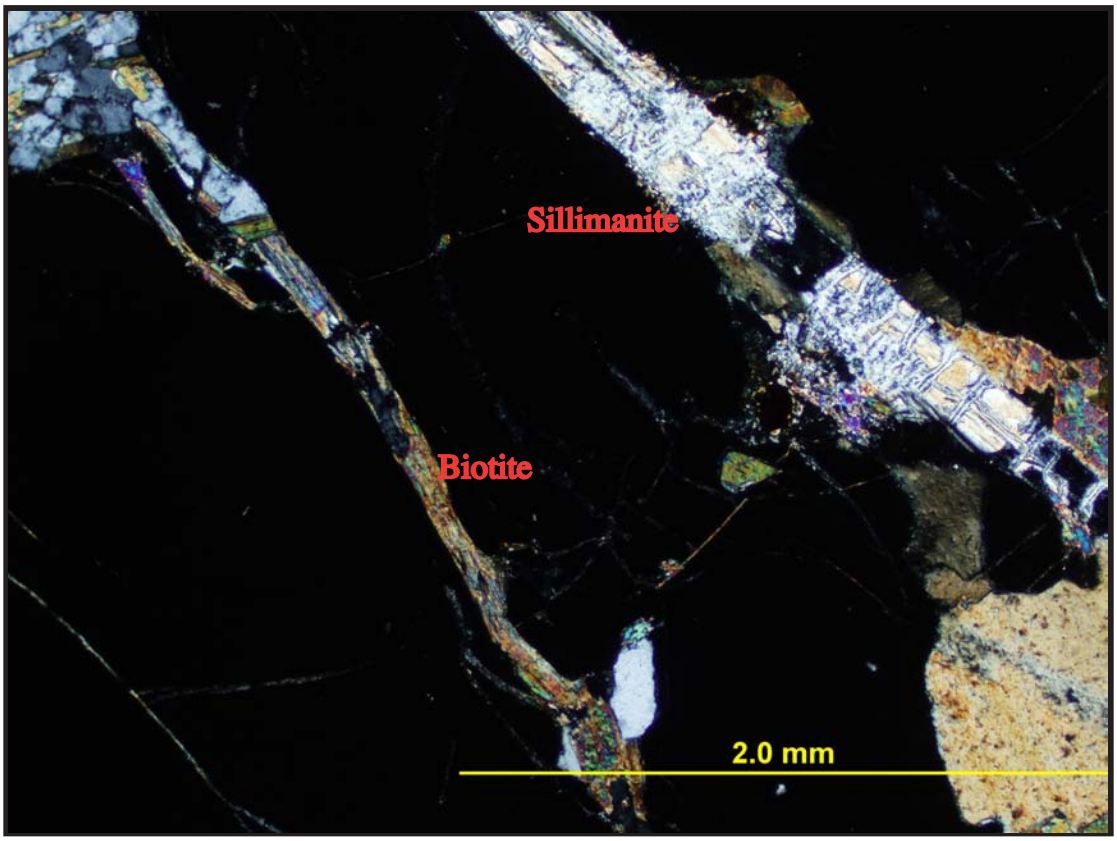

Figure 13: Photomicrograph of sample DG-8a (Camp Creek). Garnet (black) with biotite and sillimanite growing in fractures. Thin section in x-polarized light.

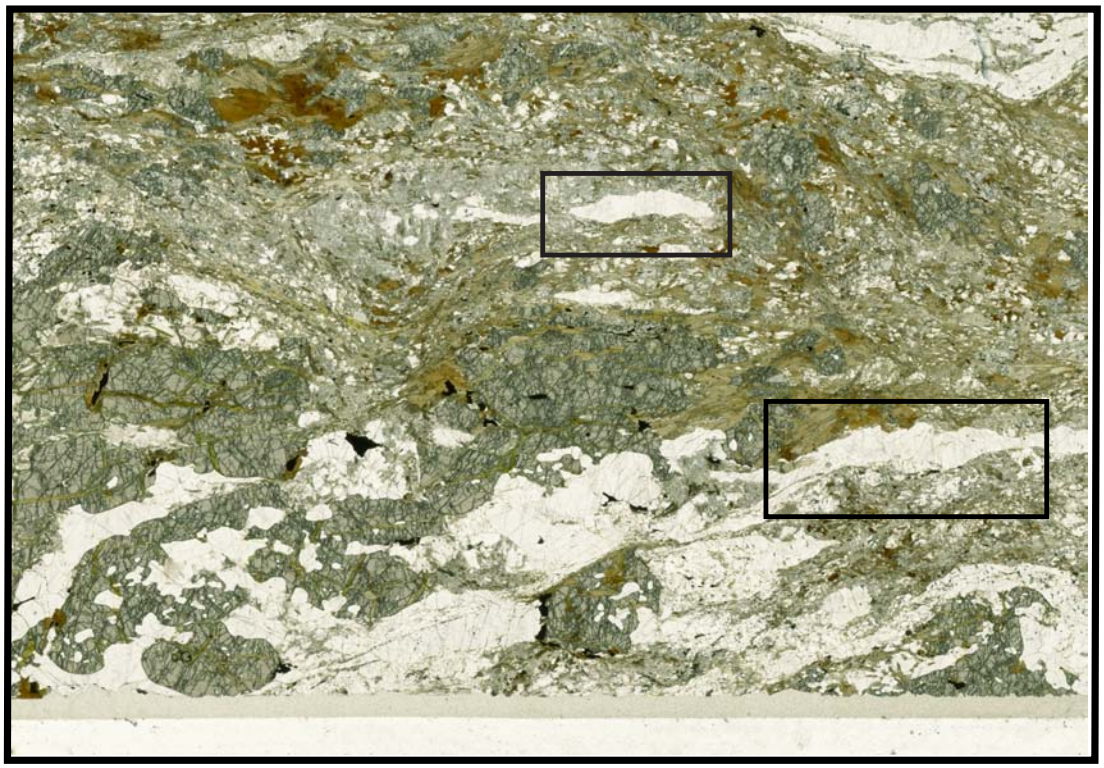

Figure 14: Sample DG-6a (Camp Creek). Lens shaped partial melt(?) containing quartz, and/or microcline and plagioclase.

CHAPTER 4: GEOTHERMOBAROMETRY

METHODS

In many samples the mineral assemblage is enough to constrain the minimum temperature and pressure that the rock must have reached at the height of its metamorphic path to a small range of possibilities, but some assemblages do not constrain conditions very well. Two samples (DG-2a from O'Neill's Gulch and DG-35b from the Ruby Range) were compositionally analyzed for garnet-biotite-quartz-plagioclase thermobarometry using the scanning electron microscope (SEM) at Smith College (SEM data analyses used for this purpose can be found in the appendix). For the samples with the assemblage garnet-biotite-quartz-plagioclase-aluminosilicate, pressures and temperatures were constrained. The program used for these calculations was Spear and Kohn's Program Thermobarometry (2001 version, available on Spear's website- see references). For the biotite-garnet exchange thermometer the Ferry and Spear (1978) calibration modified by Berman (1990) was used. Pressures were obtained using the Hodges and Crowley (1985) garnet-plagioclase barometer. Results were not calculated using the Fe^{3+} correction, since this produced results that plotted off the chart (too low) and made little sense for the mineral assemblage of the rock.

RESULTS

In general, the results of geothermobarometry calculations are extremely variable and do not constrain pressure-temperature conditions very well. Furthermore, the results do not seem to vary systematically; that is, the analyses of garnet rims and biotites in

contact seem to give the same range of variation as analyses of biotite inclusions and the adjacent garnet near the core of the garnet.

Sample DG-35b (Ruby Range) contains garnet, biotite, and sillimanite. For this sample, temperature results range from about 475-685°C. Pressures were even more poorly constrained, ranging from about 1.8-5.8 kb (Fig. 15). Mineral rim chemical analyses of a sample from O'Neill's Gulch (DG-2a) yield temperatures ranging from < 400 to about 540°C and pressures of <1.7-3.75 kb (Fig. 16).

The lower bounds of these calculated pressures and temperatures are much less than those expected based on the mineral assemblage of the rocks (i.e. the presence of sillimanite). This could be due to re-equilibration of the Mg and Fe atoms between the biotite and garnet as the rock cooled. Garnet composition varies throughout the garnet, and typically the rims of the garnet are Fe-rich. The variation of the composition makes it problematic to use the garnet-biotite exchange thermometer because it is difficult to be sure which composition represents the equilibrium composition at the height of metamorphism.

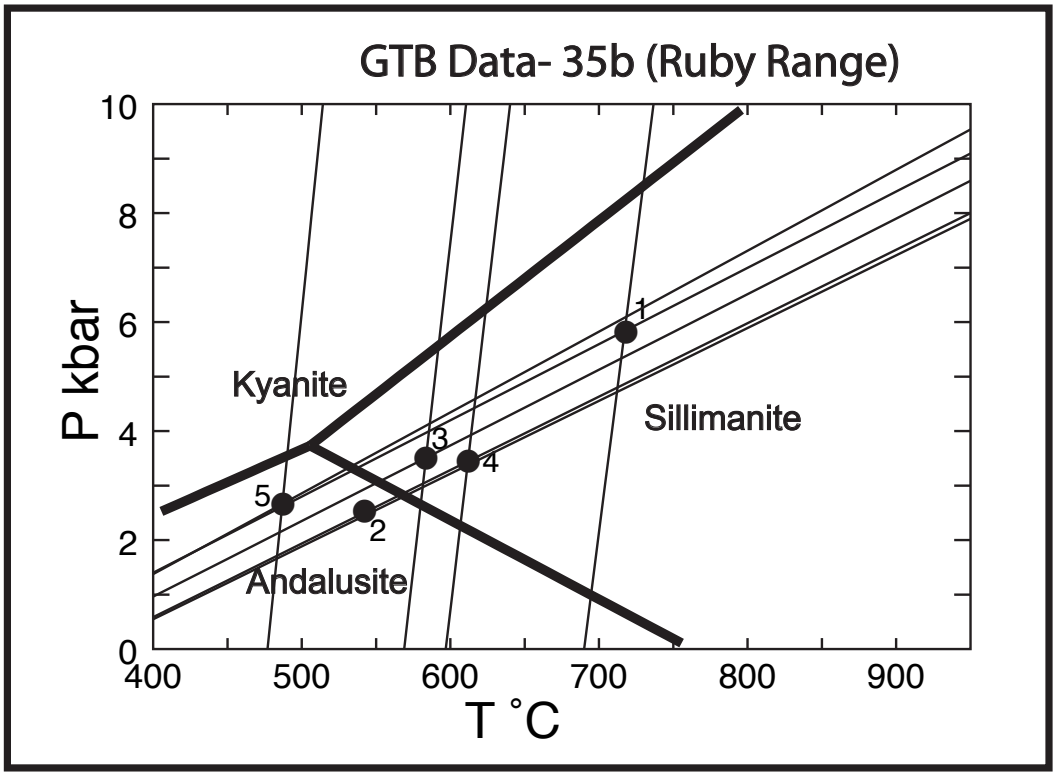

Figure 15: Geothermobarometry calculation results for sample DG-39b (represented by the black circles.) The size of the circles does not represent the error margin, which was not calculated. The data are variable and do not constrain PT conditions well.

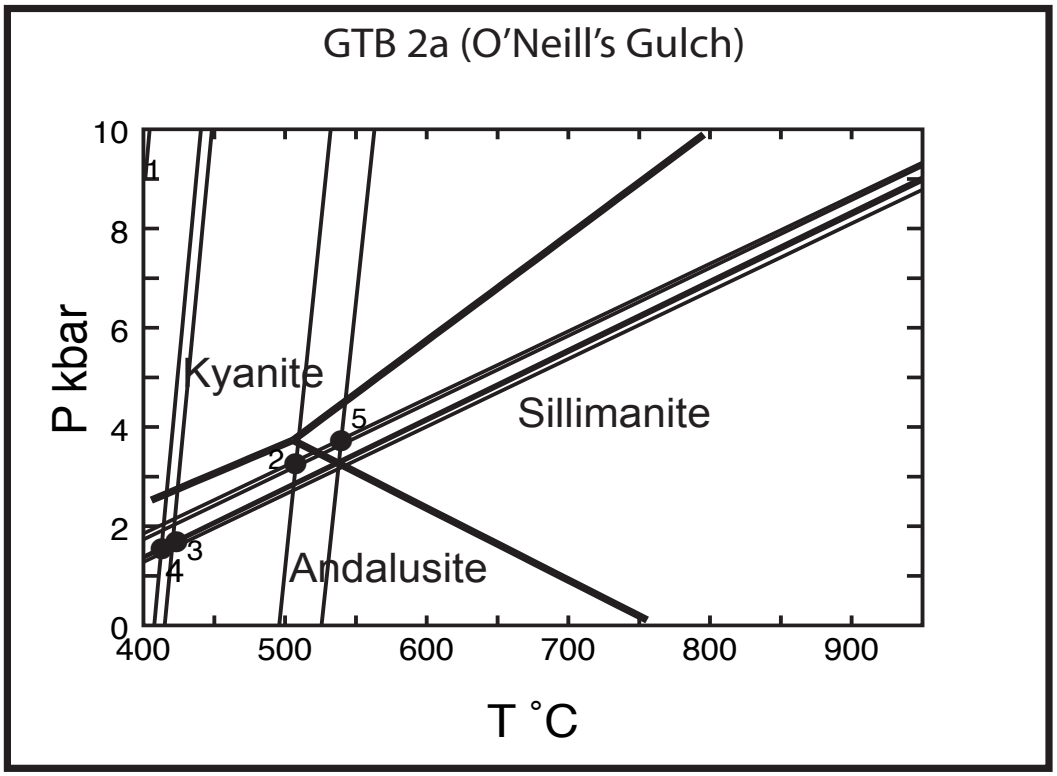

Figure 16: Geothermobarometry calculation results for sample DG-2a (represented by the black circles.) The first analysis plotted out of bounds and can be seen at the upper left. Data are variable and do not constrain PT conditions well. The size of the circles does not represent the error margin, which was not calculated.

CHAPTER 5: AGE DATING

METHODS

Two samples were dated using Th-Pb isotopic analysis of monazite, one from Camp Creek in the Highland Range (DG-8a) and one from Wall Creek (DG-29) in the Gravelly Mountains. The samples were sent to the University of Massachusetts Microprobe facility and analyses were done under the supervision of Michael Jercinovic. A reference map was made of each thin section showing the base elements Mg and Al and the rare earth element Ce. The Ce is concentrated in the monazites, which makes them easy to find within the samples (Figs. 17a and b). Monazites were selected from the sample to be dated and element maps of the monazites were made, showing Y, Ca, Th and U. These high-resolution maps show zoning (if present) in the monazite crystals (Figs. 18a and b). Points are selected from the different zones in the monazite, which "can be linked to microstructure, metamorphic minerals or metamorphic reactions, allowing specific timing constraints to be placed on stages in the structural or metamorphic history." "[The]…compositional domains are typically interpreted in terms of generations of monazite growth" (Williams et al., 2006). For my samples, zoned monazites were dated in the rim and in the core. The isotopic ratios of U, Th, and Pb were calculated and used to determine the date at which the specific part of the monazite grew (Williams et al., 2006, see also the UMass microprobe website: http://www.geo.umass.edu/probe/Monazite%20techniques-summary%20frames.htm). Data tables with results can be found in the appendices.

DEG-29 Full Section: Ce and Mg

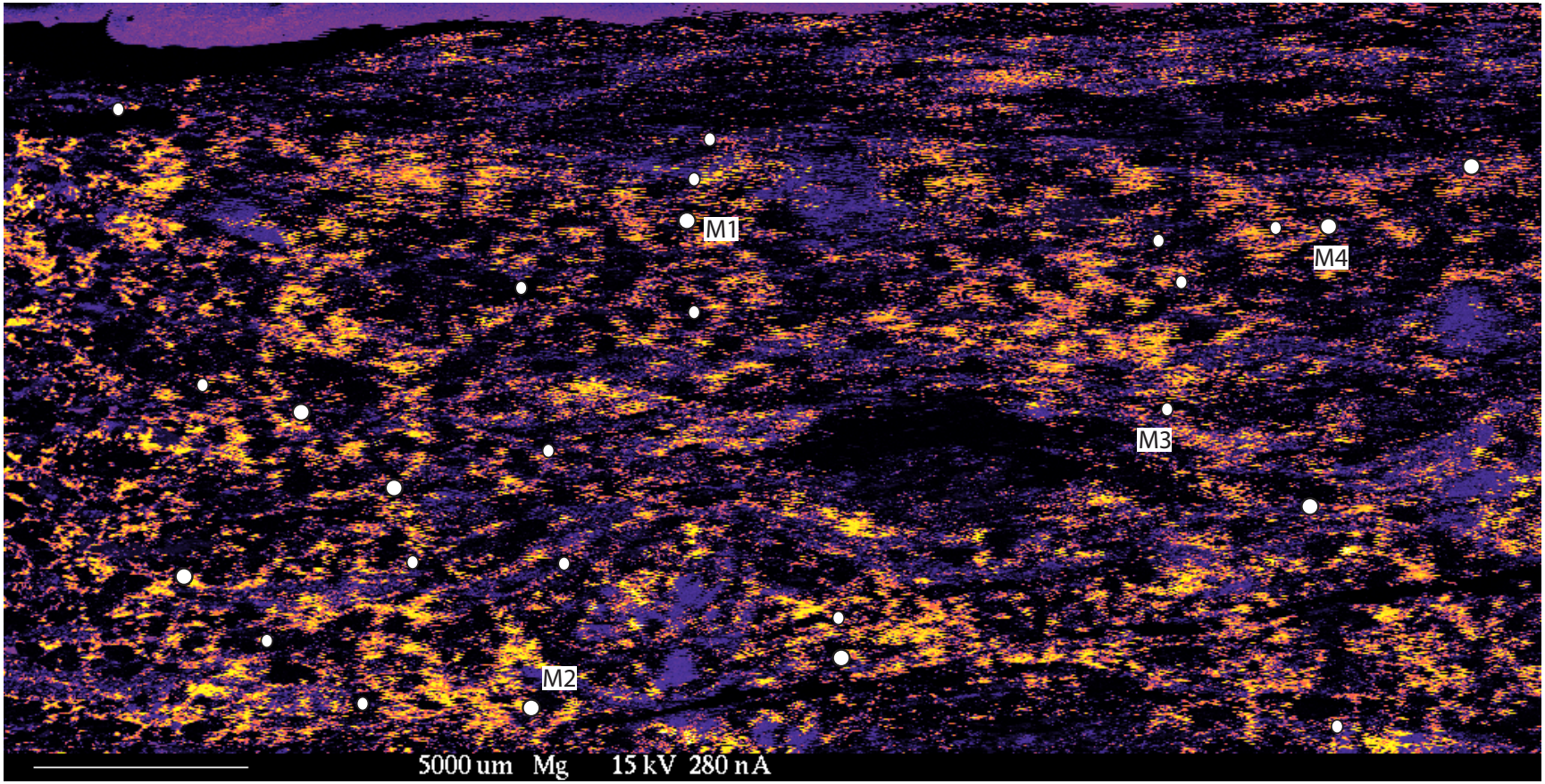

1024 X 512 step size: 35 μ ○ Ce

Figure 17a: Full section map of sample DG-29. Mg is the background map and Ce is represented by the white circles. Monazites analyzed are marked (M1-M4).

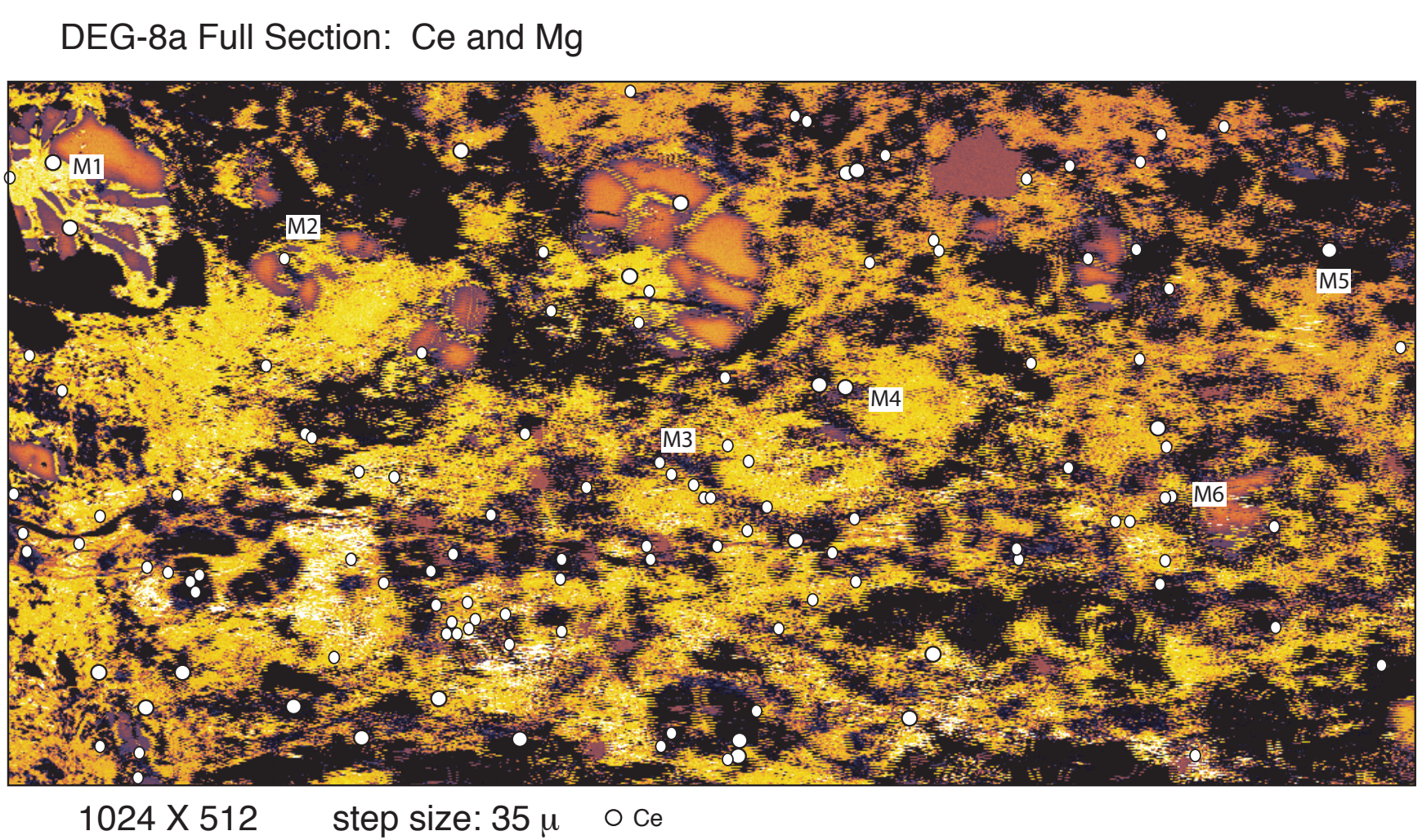

Figure 17b: Full section map of sample DG-8a. Mg is mapped in the background. Ce concentrations are represented by the white circles. Monazites analyzed are numbered (M1-M6).

Figure 18a: Compositional maps of individual monazites analyzed in sample DG-29. Four were mapped (M1-M4). The maps show relative concentrations of Y, Ca, Th and U.

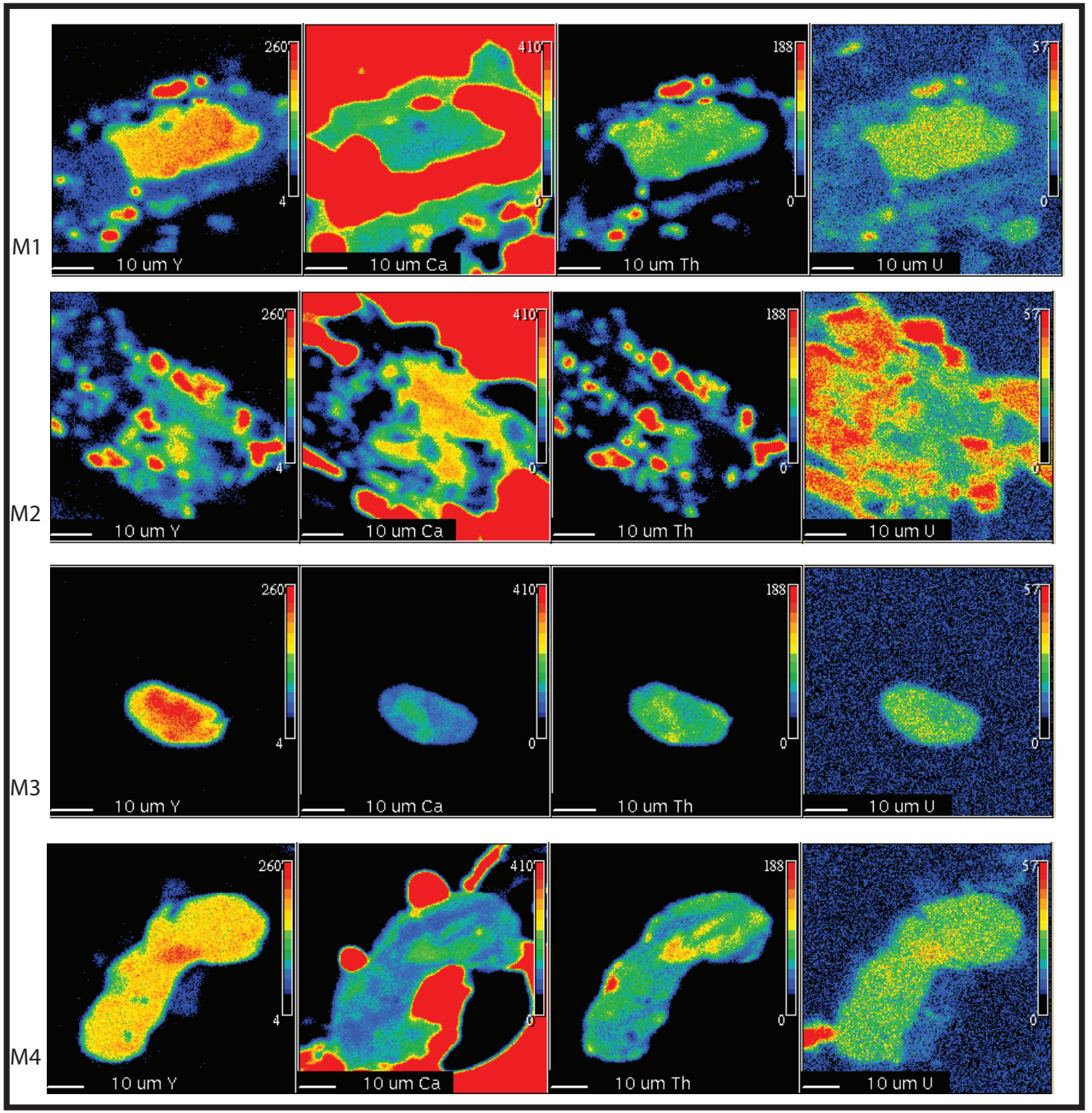

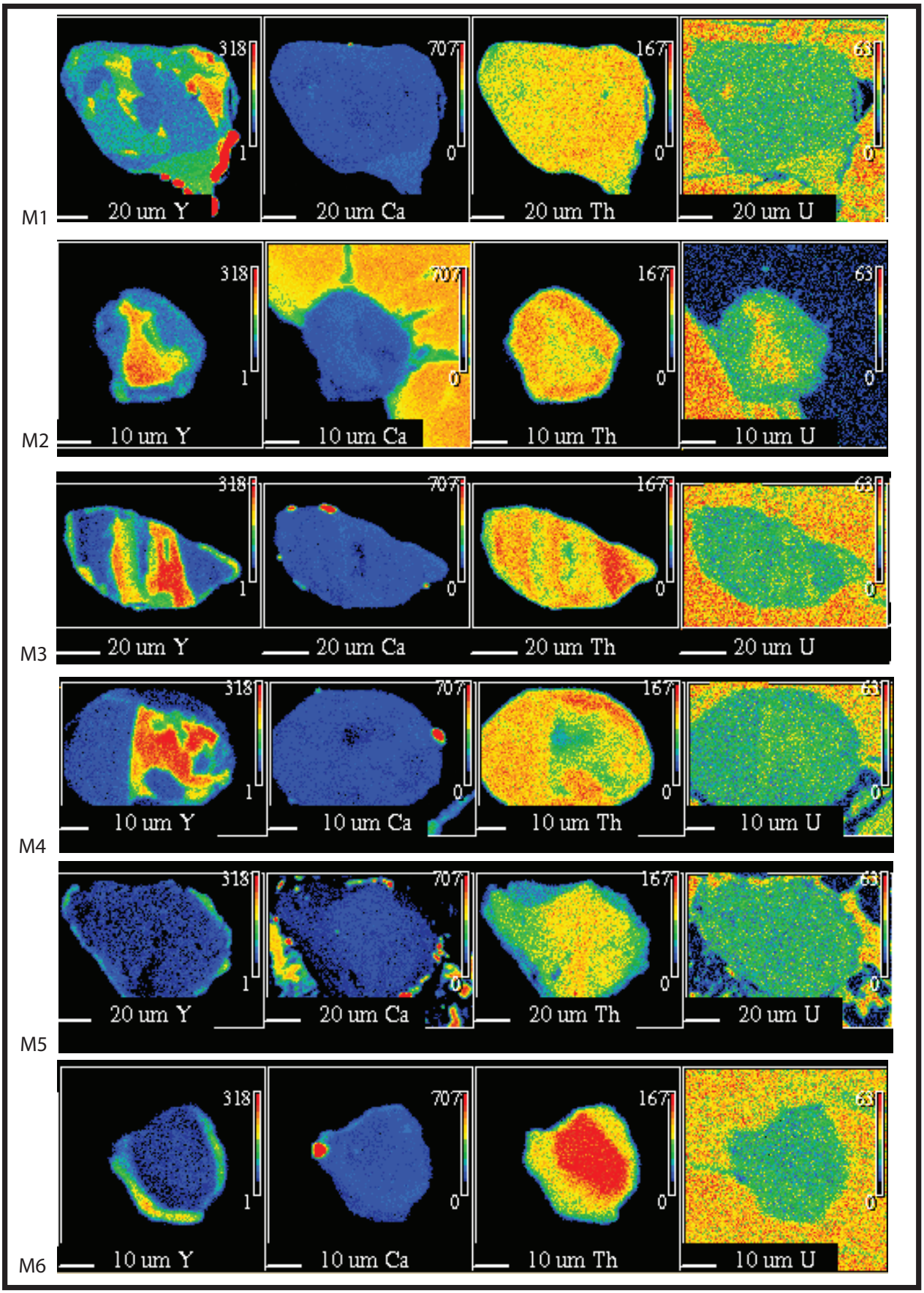

Figure 18b: Compositional maps showing concentrations of Y, Ca, Th and U in individual monazites analyzed from sample DG-8a (Camp Creek). Each monazite is numbered (M1-M6).

RESULTS

Three metamorphic monazites were dated from sample DG-29 (Wall Creek). This sample has provided a possible PT path for the Wall Creek area (see Chapter 4 and Chapter 6). The mean age for monazites analyzed in this sample is 2569 ± 45 Ma. The data are shown as Gaussian curves representing the normal distribution calculation based on the standard deviation and the mean ages (Fig19a and b).

From sample DG-8a (Camp Creek) six monazite cores and three rims were dated. The analyses resulted in two age ranges (Fig 20a and b). Most monazite analyses show a mean age of 1819 ± 28 Ma. Two monazite cores show younger ages with a mean age of 1737 ± 69 Ma (see appendix). The large standard deviation of the younger date is due to one analysis (M2 core) having a very large standard deviation of 100 Ma. Another problem with this analysis is that the mean core age (1735 ± 100 Ma) is much younger than the mean age of the rim (1812±44 Ma), though still within error. Because of the incongruence with these chemical age data, perhaps the M2 core analysis should not be considered. However, because the analysis of M6 core also shows a younger age (1739 ± 23 Ma), and because they are both core analyses and not rims, it is possible that the ages represent two periods of monazite growth, one at about 1820 Ma and one at about 1740 Ma.

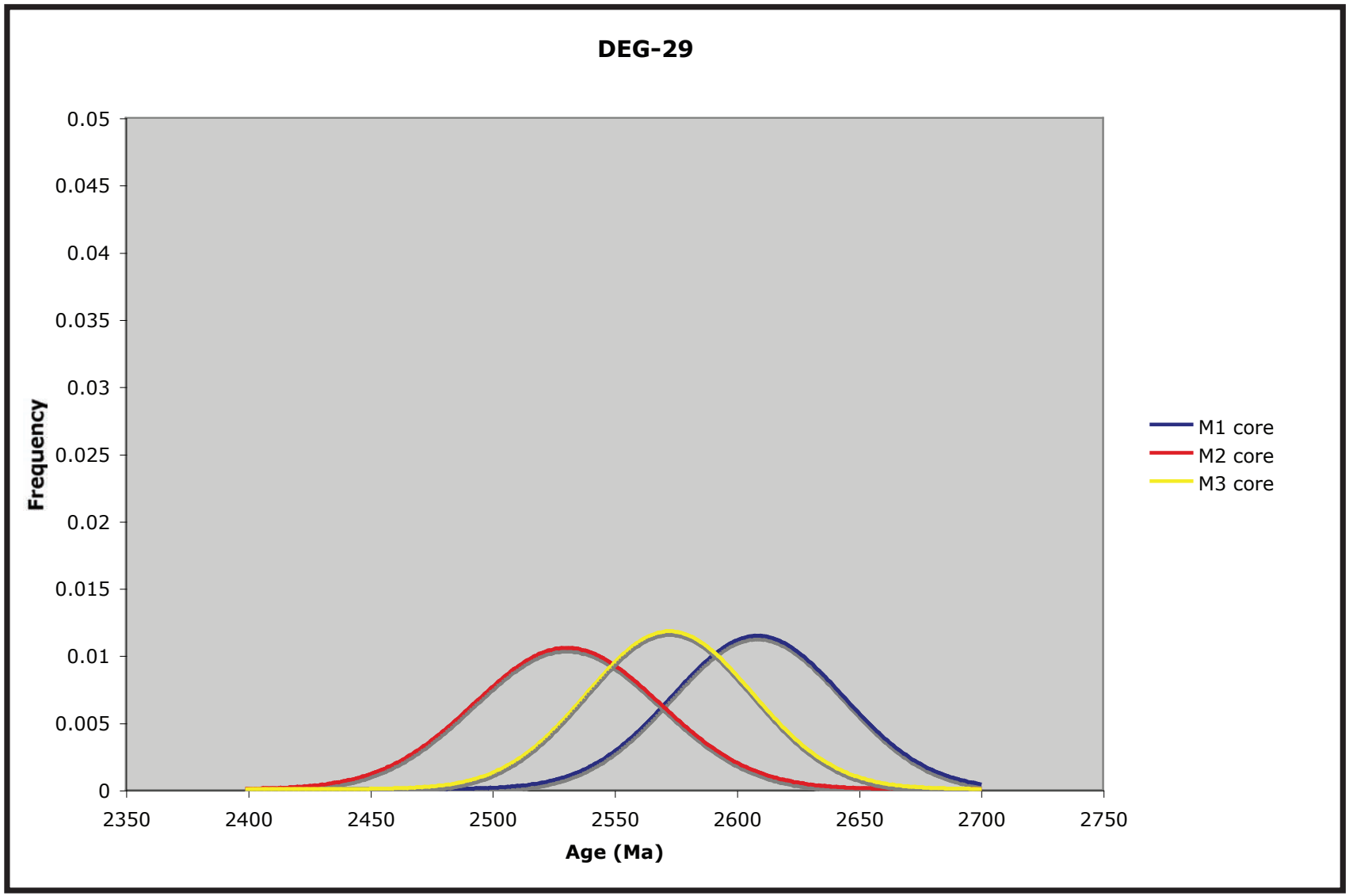

Figure 19a: Gaussian curve representing the normal distribution calculation based on the standard deviation and the mean ages for sample DG-29 (Wall Creek). The peaks represent the mean age, and the breadth of the curve indicates deviation from the mean. The mean age of all three analyses is 2569 ± 45 Ma.

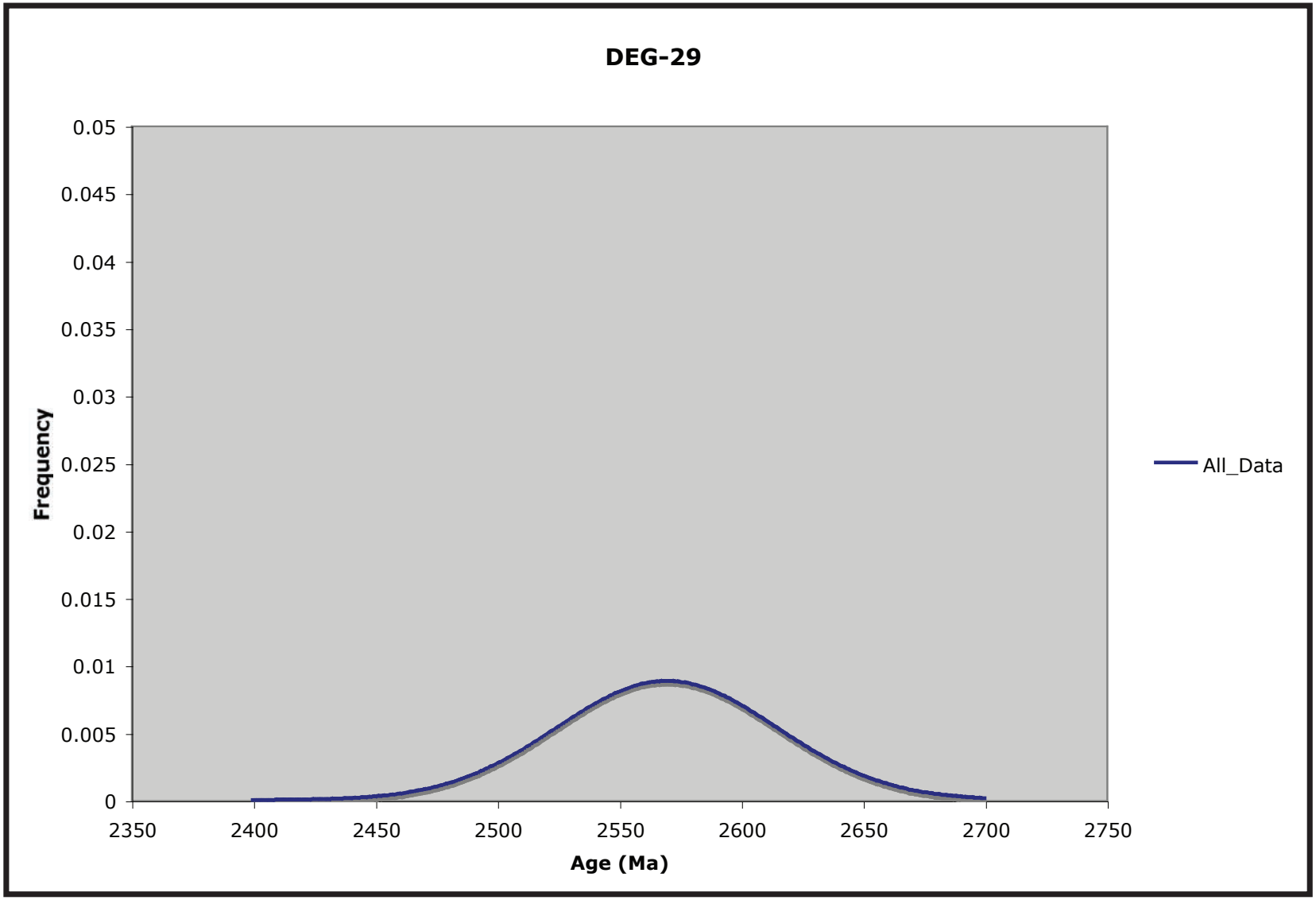

Figure 19b: Gaussian curve representing the normal distribution calculation based on the standard deviation and the mean ages for all three analyses from sample DG-29 from Wall Creek. The peak represents the mean age (2569± 45 Ma); the width represents the deviation.

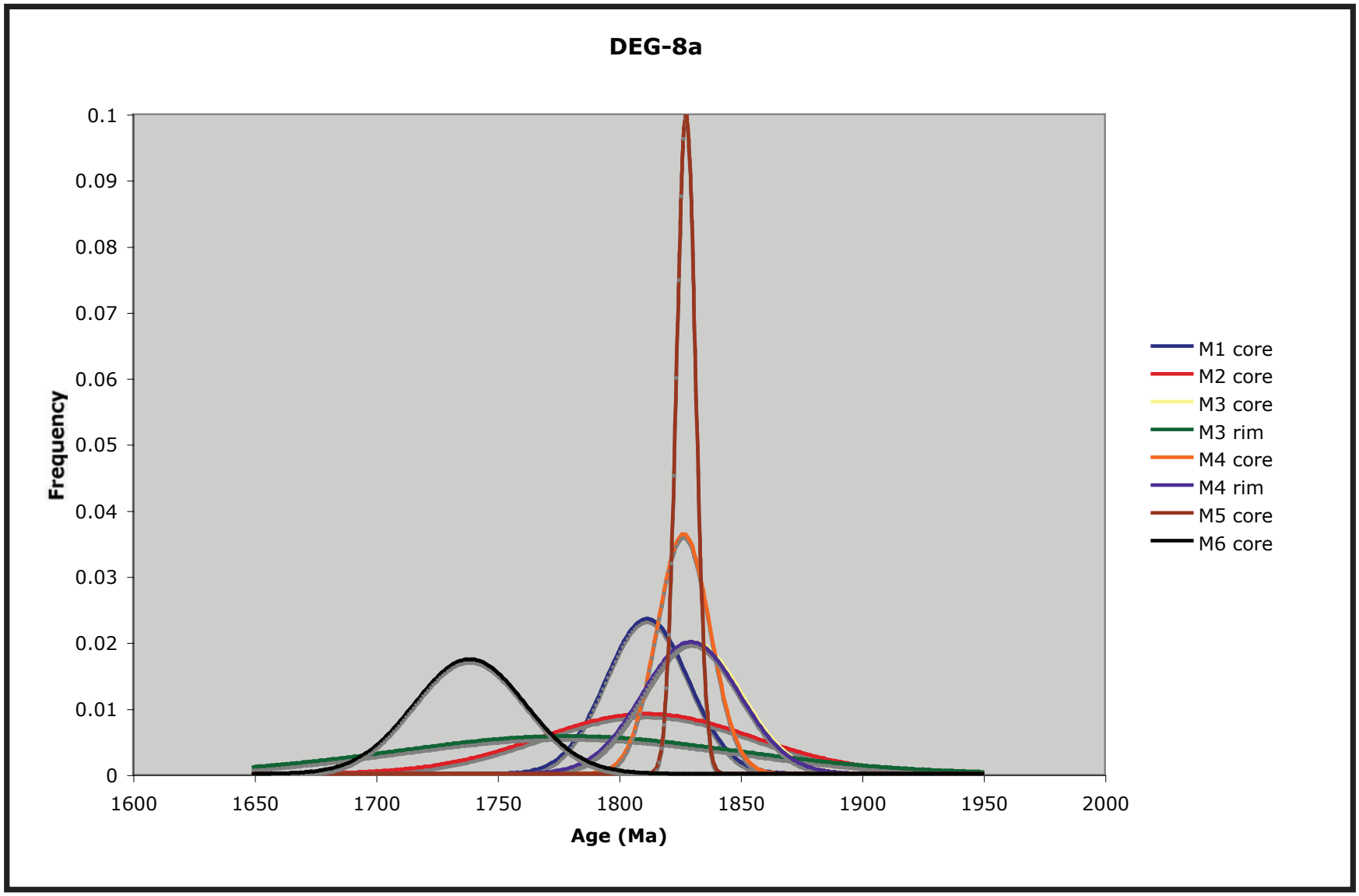

Figure 20a: Gaussian curve representing the normal distribution calculation based on the standard deviation and the mean ages for each point analyzed in sample DG-8a. The peak represents the mean age, the width represents the standard deviation.

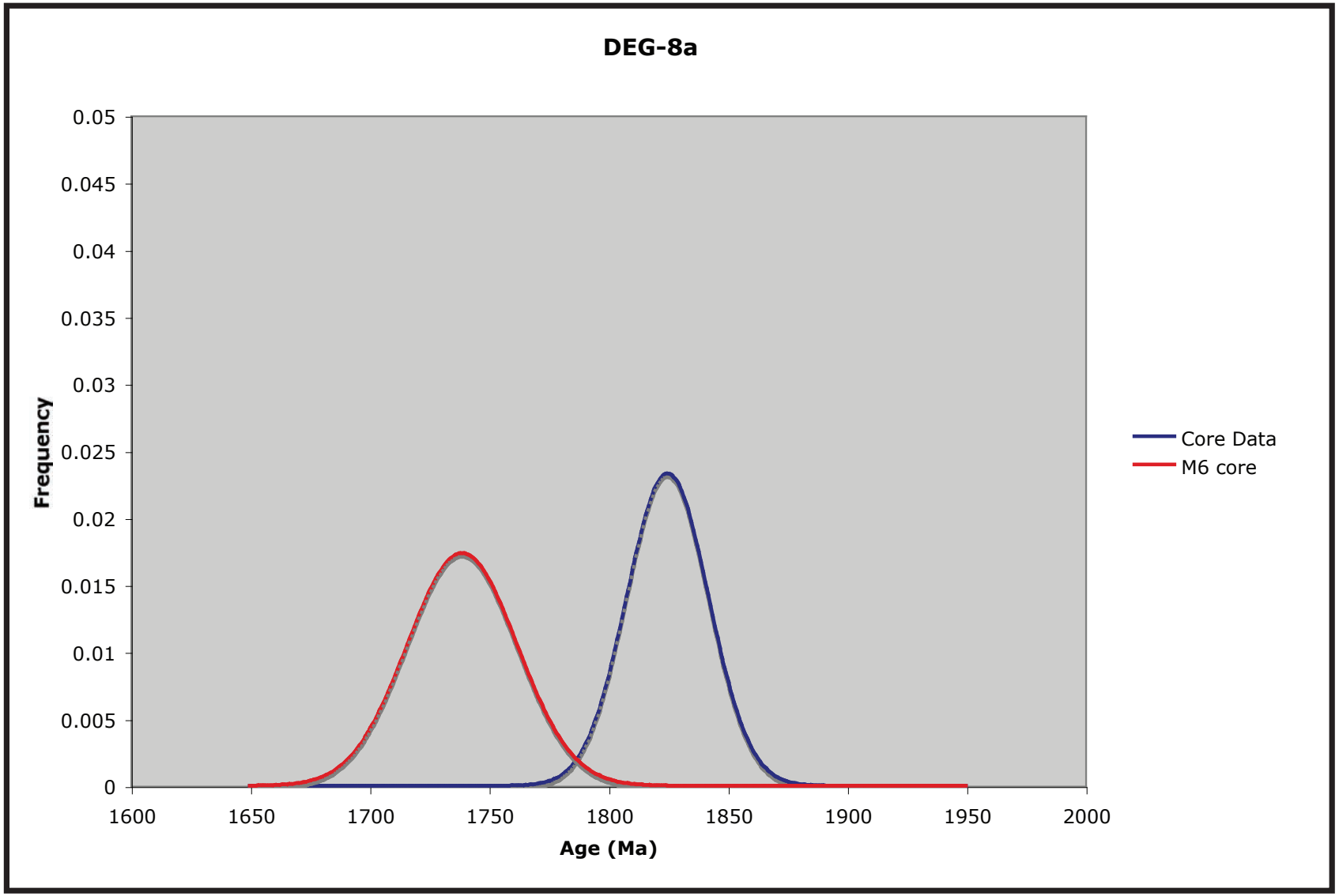

Figure 20b: Gaussian curve representing the normal distribution calculation based on the standard deviation for all analyses. This shows the mean age of all data in sample DG-8a (blue) except M6 core (red) which gives a much younger mean age.

CHAPTER 6: RESULTS, DISCUSSION, AND CONCLUSION

RESULTS

Gravelly Range

In general, metamorphism seems to be lower grade in the Gravelly Range than in the Highland or Ruby Ranges. This is based on the presence of andalusite, and lack of migmatitic textures.

Of all areas studied, the Luzenac Mine area seems to be the area of least metamorphism. Depositional bedding planes are preserved in phyllite and quartzite. Also, no minerals were identified that would suggest high-grade metamorphic facies. It seems very unlikely that original cross bedding could be preserved in the quartzite or fine-scale bedding in the phyllite had the area undergone significant deformation and/or metamorphism.

In contrast, the Wall Creek area of the central Gravelly Range shows a very complex metamorphic history. Rather than reflecting just one metamorphic grade, evidence from this area suggests a path of metamorphism. Bundles of prismatic kyanite pseudomorphed after andalusite, observed in sample DG-32a, indicate an increase in pressure. A sample of phyllite from just a few meters away (DG-29) shows kyanite, fibrous sillimanite and a crystal with inclusions that are reminiscent of andalusite's characteristic chiastolite cross in close proximity in a single thin section (see Fig. 8). The kyanite appears relict, with sillimanite growing around it. It seems reasonable to speculate that the crystal containing the inclusions is a kyanite pseudomorphed after andalusite as observed in sample DG-32a discussed above. The inclusions in the crystal are not graphite as would be expected, but they are concentrated in the center of the

crystal and give the appearance of andalusite. Even if the crystal is not andalusite, together these two samples suggest a single metamorphic event following a clockwise PT path around the triple point, with andalusite forming first, then kyanite and finally sillimanite (Fig. 21). The reason to believe that it was a single event and not the result of more than one event is because the monazites from DG-29 give only one age (2569±45 Ma). Another sample from the area contains prismatic and fibrous sillimanite, as well as staurolite and biotite. Based on this mineral assemblage, the PT path established for this area must have reached temperatures of at least 540 °C and pressures of at least 3 kb (Spear, 1993).

Standard Creek rocks generally show lower grade assemblages than those from Wall Creek, where the rocks reached at least amphibolite facies. Most rocks in Standard Creek are greenschist or epidote amphibolite facies and contain andalusite, staurolite, and biotite. The only sample containing evidence of a higher-grade of metamorphism was DG-44, which contained a small amount of fibrous sillimanite, placing the rock in amphibolite facies. It should be noted that, although samples came from at least 460 meters from the Standard Creek metagabbro pluton, the subsurface extent of the pluton is not well known. Therefore, the possibility of contact metamorphism should be considered as well as the extent of regional metamorphic events.

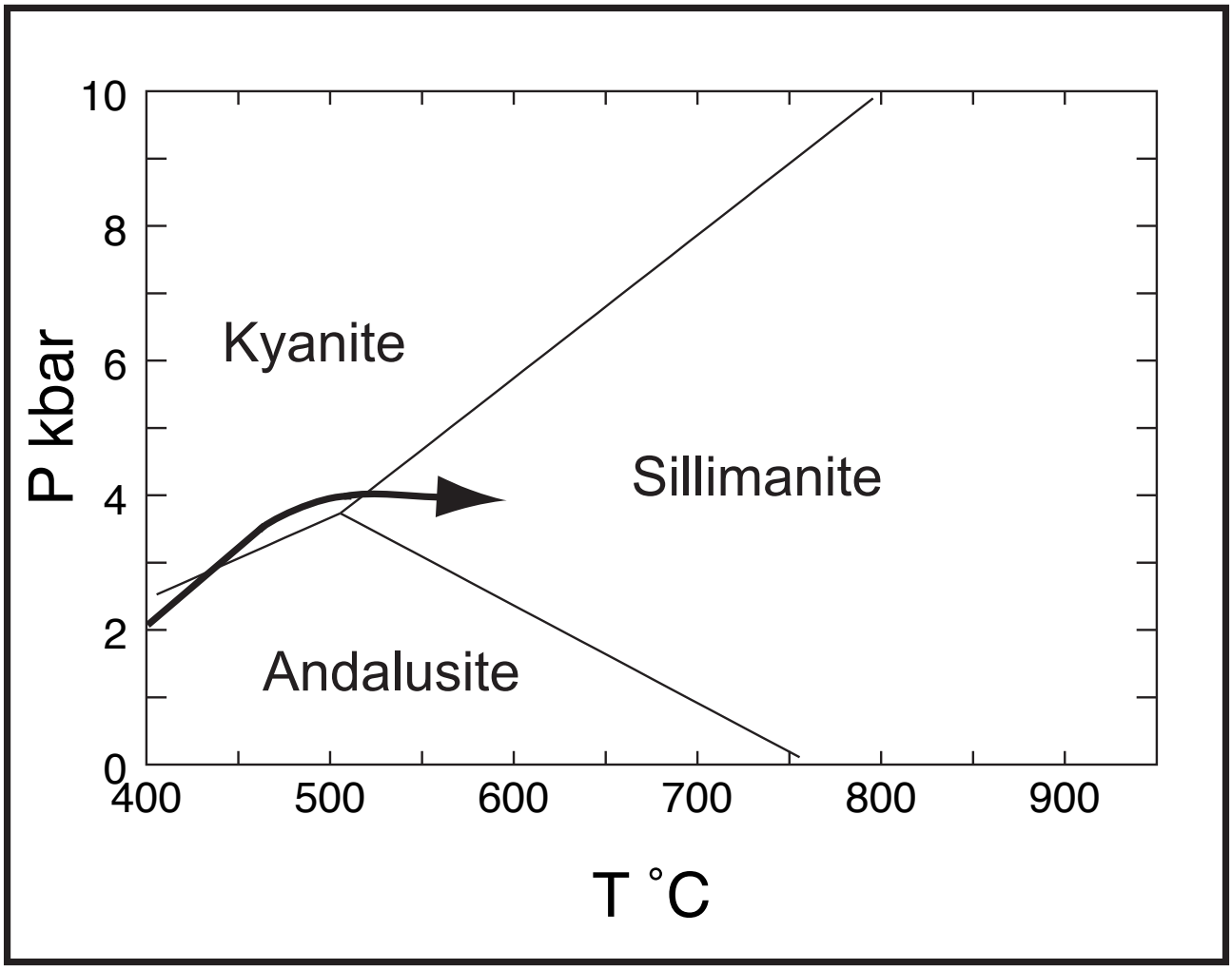

Figure 21: Schematic pressure-temperature path for Wall Creek based on samples DG-29 and DG-32a, passing from andalusite to kyanite and finally to sillimanite zone conditions in a clockwise path.

Ruby Range

The Ruby Range shows signs of high-grade metamorphism. Two samples examined in thin section from the Ruby Range have the assemblage biotite-garnet-sillimanite, giving a minimum temperature of about 550°C and pressures from about 2.5 to 6.25 kb (Spear, 1993). The geothermobarometry calculations were not very helpful in determining metamorphic grade for the Ruby Range because the results vary so much (see Chapter 4). The mineral assemblage, however, successfully constrains metamorphism to amphibolite facies.

Dahl (1980) found sillimanite and potassium feldspar bearing rocks with no stable prograde muscovite in the Ruby Range. This is evidence that, at least in some places, metamorphism in the Ruby Range crossed the reaction isograd: muscovite + quartz → alumino-silicate + k-feldspar. The reaction occurs at a minimum of 500 degrees C in the andalusite zone, but temperatures of about 600 degrees C are required in the sillimanite zone (Spear, 1993). In some metapelites relict kyanite was found (Dahl, 1980). Thus, a metamorphic P-T path passing from the kyanite stability field and then into the sillimanite field was postulated by Karasevich et al. (1981). They also found that metamorphic conditions were higher in the northern third of the Ruby Range than elsewhere within the range, based on orthopyroxene-zone assemblages that were not found elsewhere in the range (Karasevich et al., 1981).

Highland Range

The Highland Mountains, like the Ruby Range, show evidence of high-grade metamorphism, with many samples containing sillimanite. In O'Neill's Gulch both prismatic sillimanite and fibrolite occur, in some cases within the same thin section.

Only prismatic sillimanite is present in thin sections from Camp Creek. In one sample from each location, microcline is present. The sample from Camp Creek (DG-6a) contains no muscovite, indicating that metamorphism in this area of the Highlands crossed the reaction isograd muscovite + quartz→ potassium feldspar + aluminosilicate. This constrains the temperature of metamorphism to at least 600°C (Spear, 1993; see also Labadie, 2006). The sample from O'Neill's Gulch contains microcline, sillimanite and muscovite, so perhaps the reaction began but was not completed. Based on evidence from these two samples it appears that Camp Creek experienced either higher temperatures or lower pressures than O'Neill's Gulch, though muscovite seems stable in some samples from both areas. Mineral rim chemical analyses of a sample from O'Neill's Gulch were not helpful in determining temperatures and pressures of metamorphism. Results yield temperatures ranging from < 400 to about 540°C and pressures of <1.7-3.75 kb -- much lower than those expected based on the mineral assemblages present (see Chapter 4). Like the Ruby Range, I believe that these low results are due to re-equilibration of the Mg-Fe exchange between garnet and biotite during cooling.

DISCUSSION

The grade of metamorphism is highly variable between the mountain ranges in the northern Wyoming province and there is a general trend of increased temperature in the northern ranges (Fig. 22). The highest grade of metamorphism (upper amphibolite to granulite facies) is recorded by rocks in the Highland and Ruby Ranges. Rocks near the Luzenac mine in the northern Gravelly Range show the lowest grade of metamorphism.

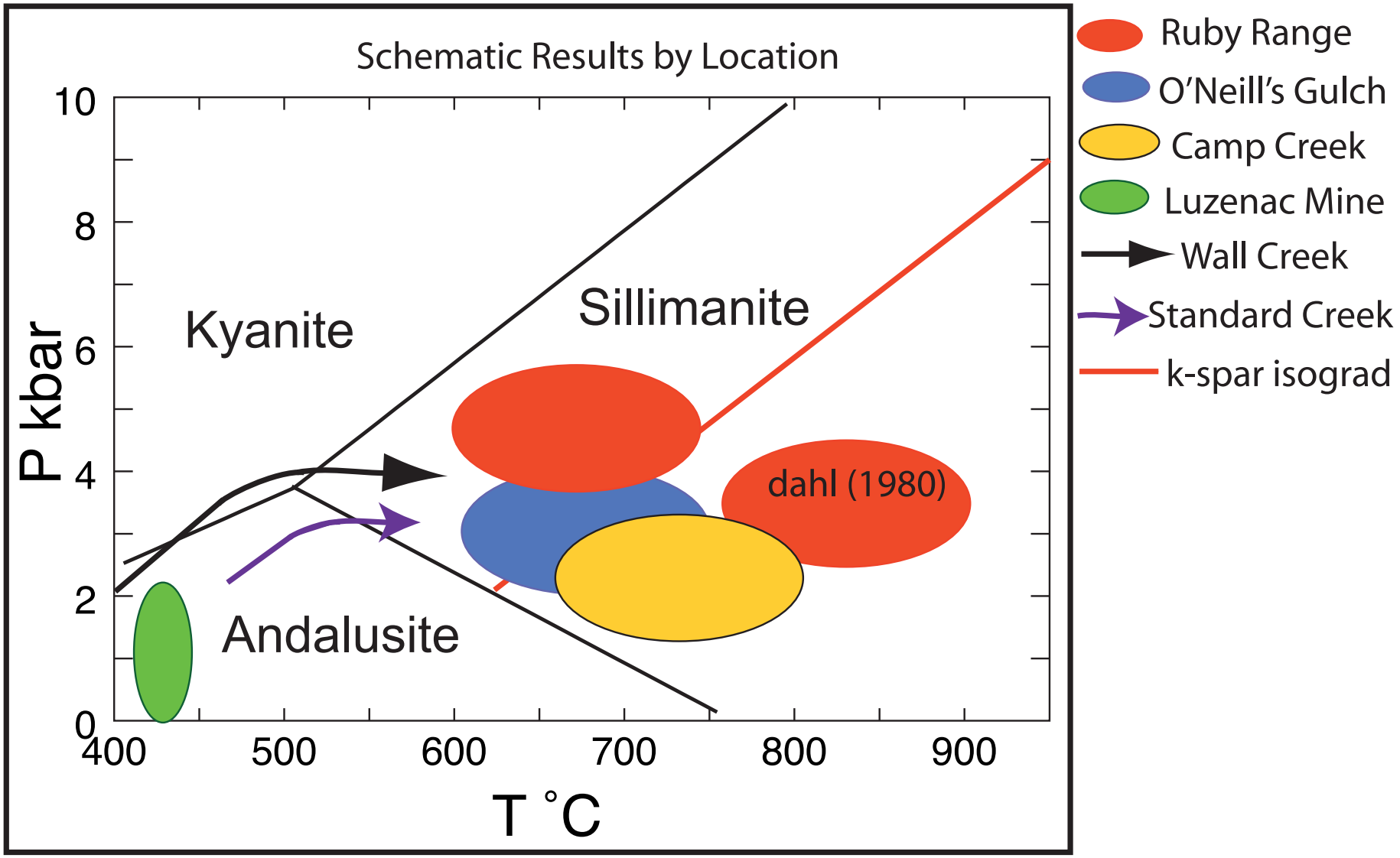

Figure 22: Schematic pressure-temperature zones and possible PT paths for each location studied, based on PT minimums determined. For the Ruby Range minimum pressures and temperatures determined by this study are 550 degrees C and 2.5 kb, so it is possible that they are congruent with the results of Dahl (1980). Result ellipses show the approximate metamorphic conditions that samples from this study may have experienced based on petrology. For more detailed information, see Chapter 7.

The metamorphic history of the Gravelly Range is the most complicated. Each area studied in the Gravelly Range shows a metamorphic history that is very different from the history of the Highland and Ruby Ranges and also very different from the other areas studied within the Gravelly Range.

The difference in metamorphic grade between the northern ranges (Ruby and Highland) and the Gravelly Range could be explained by the different ages obtained from monazites. The major metamorphic event in the Highland Range during which monazite grew occurred at 1819 ± 28 Ma. The two monazite analyses that show younger ages (1737 ± 69 Ma) may represent a second, less intense, metamorphic event (see appendices and Figures 20a and b for age analyses of the Highland Range Sample DG-8a). These ages are relatively close to dates already established in other areas of the northern Wyoming Province, including the Tobacco Roots, for the Big Sky orogenic event (occurring at about 1770-1713 Ma) (Cheney et al., 2004). Therefore it seems reasonable to conclude that the metamorphic grade observed in the Highland Range is a result of the Big Sky orogeny. Similar grade of metamorphism observed in the Ruby Range and the fact that the lithologies of the Ruby Range and the Highland Range are similar (Wilson, 1981) suggest that the Ruby and Highland Range metamorphisms are related and therefore are both a result of the Big Sky orogeny.

Although it seems clear that the ages in the Highland Mountains reflect Big Sky metamorphism, the Highland ages are significantly older (perhaps 50 Ma) than the ages recorded in the Tobacco Roots. Matthews (2006) also found older monazite ages (1806 ± 24 Ma and 1856 ± 21 Ma) in some samples from O'Neill's Gulch in the Highland Mountains as well as ages characteristic of Big Sky metamorphism (about 1717-1761

Ma). The large range in dates is curious. The differences in ages could be due to monazite growth that is not necessarily reflective of the major metamorphism, since zoning of the rare earth element Y in monazite can occur as a result of the breakdown of garnet (see Fig. 18b for zoning). This happens because garnet can also contain Y in its crystal structure and as the garnet breaks down the Y is released and can then be used in monazite growth. It is possible that some of the monazite rims are rich in Y for this reason (Matthews, 2006; see also Mahan et al., 2006). The different ages of the monazites could be a result of these complexities.

A second possible explanation for the fact that monazite ages in the Highlands are older than those recorded in the Tobacco Roots is the difference in location. The Highland Range is located to the northwest of the Tobacco Root Mountains and it is possible that the Highland Range experienced metamorphism before the Tobacco Root Mountains due to the nature of the collision during the orogenic event. If the collision came from a more north or northwesterly direction, it makes sense that the Highland rocks would record older metamorphic ages than rocks from the Tobacco Roots.

Monazites from the Wall Creek area of the Gravelly Range give an age of 2569 ± 45 Ma. This explains the contrast in metamorphic grade as compared to the northern ranges since the major metamorphism must be due to a completely different event. Cheney et al. (2004) report ion microprobe monazite dates from the Tobacco Root mountains that range from 2439 ± 25 to 2451 ± 22 Ma. Although the Wall Creek dates are somewhat older, they are most likely related to this previous metamorphic event, which has also been interpreted as orogenic in nature. Other indications of this event have been found in the region, including zircon dates from the Tobacco Root mountains

and the presence of a gneissic fabric that is cross-cut by MMDS that intruded around 2060 Ma (Cheney et al., 2004, see also Harms et al., 2004).

Temperatures high enough to grow sillimanite would presumably grow new monazites or rims on the pre-existing monazite crystals. Based on this assumption it seems clear that the sillimanite found in Wall Creek and in Standard Creek is not due to the Big Sky orogeny, since no monazites from either location date younger than the ca. 2550 Ma event (Doody, personal communication).

The presence of sillimanite in sample DG-44 from Standard Creek is curious because it is not found in any other samples from the area, all of which reflect andalusite zone metamorphic conditions. A possible explanation is that the rocks in Standard Creek underwent metamorphism at conditions very near those required to transition to the sillimanite zone. Only in some areas was the initial energy present that is required to complete the reaction.

Another possibility is that the Standard Creek rocks, like Wall Creek rocks, are demonstrating evidence of a metamorphic path passing from the kyanite to the sillimanite zone. This path could possibly parallel the Wall Creek path, but at lower pressures (see Fig. 22). Rocks in the Gravelly Range generally dip to the north, so structurally rocks in Standard Creek are below Wall Creek rocks. Therefore one would expect Standard Creek rocks to display higher pressure conditions with respect to Wall Creek rocks rather than the lower pressure conditions observed. This apparent incongruity could be explained by the possible structural and perhaps tectonic boundaries in the Gravelly Mountains (Vargo, 1999; see also Klein, 2006). At the time of metamorphism, Standard Creek rocks could have been located above Wall Creek rocks, explaining the congruent

PT paths at different pressures (Fig. 22). Possibly, the Wall Creek rocks were subsequently thrust over the Standard Creek sequence after the metamorphic event that grew the sillimanite.

Giletti's line separating rocks affected by the ca. 1750 Ma event from older rocks has been postulated to run through the Gravelly Range somewhere between Standard Creek and the Luzenac Mine Area (Harms et al., 2004). The monazite ages obtained from the Gravelly Range suggest that Giletti's line lies to the north of the Wall Creek area. But Giletti (1966) used K-Ar dates of micas to determine the location of the boundary, which are reset at about 350 °C, lower than the temperatures required to grow monazite. Therefore it is possible that, if the rocks in the Gravelly Range were heated during the Big Sky event, the micas in Wall Creek could have been reset, but conditions did reach the temperatures or pressures required to grow monazite. So the boundary line could be located within the Wall Creek area somewhere, or even south of it. One indication that Wall Creek is in fact a boundary area is that shearing textures are observed in the rocks.

Important structural boundaries in the Gravelly Range, evidenced by differences in the age and character of metamorphism and also in a study of the Luzenac Area done by Klein (2006), may be related to other structural boundaries in the region. In the Madison Range, to the east of the Gravelly Mountains, there is a "wide, northeast-striking, northwest-dipping shear zone that roughly parallels Giletti's line" (Harms et al., 2004). This is the Madison mylonite zone of Erslev and Sutter (1990). "It is interpreted as a thrust fault because it places higher-grade rocks over lower-grade rocks" (Harms et al., 2004). Ar-Ar ages of rocks within this zone give ages of about 1.8 Ga (Big Sky

metamorphism) but surrounding rocks give the older Ar age of 2.4-2.5 Ga (Erslev and Sutter, 1990). The Big Sky age of the zone means that it must have been active during the Big Sky orogeny. It also parallels other shear zones in the region, which may "constitute a belt of ductile thrust faults between the Big Sky metamorphic core to the northwest and Giletti's line to the southeast that straddles the transition from the infrastructural hinterland to the supracrustal foreland of the orogen" (Harms et al., 2004). Schwab (2006) has found evidence that the Madison mylonite zone extends into the Madison River valley. It is possible that this shear zone also extends into the Gravelly Range.

The considerable variation in metamorphic grade within the range could be due to the presence of these major structural boundaries. The major boundaries may exist between the Luzenac Mine area and Wall Creek (see Klein, 2006). Wall Creek itself could be a shear zone or major fault.

The origin of the lower-grade metasedimentary rocks in the Gravelly Range is still unclear. It is possible that the sedimentary protolith of at least some of the rocks in the Gravelly Range were foreland basin deposits that were later metamorphosed and "overridden by the ductile thrust faults of the southern and northern Madison ranges" (Harms et al., 2004, see also O'Neill, 1998). If rocks from Standard Creek and from Wall Creek are indeed foreland basin deposits, they must be deposits from an orogenic event that occurred long before the Big Sky event, based on the much older metamorphic monazite ages (see Doody, 2006 and Chapter 5 of this volume). It remains a possibility that the rocks north of Wall Creek, in the Luzenac Mine area, represent the foreland sedimentary deposits of the Big Sky orogen. Age dating of detrital zircons in rocks from

this area could verify whether or not this is a possibility, as suggested by Harms et al. (2006). If Luzenac Mine rocks do in fact represent Big Sky orogen rocks, this necessitates a major boundary separating them from rocks in Wall Creek and further south. If the rocks from the Luzenac Mine area have some other origin, then perhaps the lower grade foreland basin deposits of the Big Sky orogen remain unexposed or have been eroded away.

Many questions remain regarding the metamorphic history of the area. Very little is known about the nature of the orogeny at 2550 Ma, which is the major event recorded by rocks in the central and southern Gravelly Range. Why do the Luzenac Mine rocks show a lower grade of metamorphism than meta-pelites in the southern Gravelly Range? How do the metamorphic histories of Standard Creek and Wall Creek relate to one another? What has been the effect of the numerous gabbroic intrusions on this metamorphism? Vargo (1990) gives an Ar-Ar date for micas in a rock further north in the Gravelly Range (Cherry Creek area), which reflects Big Sky metamorphism. Will the Ar-Ar dates of micas south of Cherry Creek (my study area) reflect Big Sky metamorphism, or the 2550 Ma event?

CONCLUSION

Two major orogenic events are recorded in the rocks examined for the purposes of this study. Higher-grade rocks from the Highland and Ruby Ranges to the north give clear evidence of a major orogenic event and high-grade metamorphism at around 1800 Ma (see Fig 22), an age undoubtedly attributable to the Big Sky event. The central and southern Gravelly Range show evidence for an older, lower-grade orogenic event (ca

2550 Ma), which possibly follows a clockwise PT path. No clear evidence of the Big Sky orogeny (ca. 1800 Ma) is exhibited by rocks in the central and southern Gravelly Range. The metamorphic and original depositional history remain unclear for the anomalously low-grade rocks in the Luzenac Mine area. High-grade metamorphism and Big Sky Ar ages similar to those exhibited in the Tobacco Root, Ruby, and Highland Ranges have been recorded in the Cherry Creek area of the northernmost part of the Gravelly Range (outside my study area, see Vargo, 1990).

The contrast in character of metamorphism and the difference in ages found within the Gravelly Range show that at least one major structural and/or tectonic boundary runs through the range. This boundary is possibly related to or the same as the Madison mylonite zone to the east and to Giletti's line, which separates rocks whose Ar systems have been reset during the Big Sky orogeny from rocks whose Ar systems have not. Giletti's line must run through the Gravelly Range, and it is likely that it runs through Wall Creek or just north of it.

References

Berman, R.G., 1990, Mixing properties of Ca-Mg-Fe-Mn garnets. American Mineralogist, 75, p. 328-344.

Boerner, D.E., Craven, J.A., Kurtz, R.D., Ross, G.M., and Jones, F.W., 1998, The Great Falls tectonic zone: Suture or intracontinental shear zone?: Canadian Journal of Earth Sciences, v. 35, p. 175-183.

Brady, J.B., Burger, H.R., Cheney, J.T., and Harms, T.A., eds., 2004, Precambrian Geology of the Tobacco Root Mountains, Montana: Geological Society of America Special Paper 377.

Burger, H.R., 1966, Structure, petrology, and economic geology of the Sheridan district, Madison County, Montana [Ph.D. Thesis]: Bloomington, Indiana University.

Burger, H.R., 1969, Structural evolution of the southwestern Tobacco Root Mountains, Montana: Geological Socitey of America Bulletin, v. 80, p. 1329-1342.

Burger, H.R., 2004, General geology and tectonic setting of the Tobacco Root Mountains *in* Brady, J.B., Burger, H.R., Cheney, J.T., and Harms, T.A., eds., 2004, Precambrian Geology of the Tobacco Root Mountains, Montana: Geological Society of America Special Paper 377, p. 1-13.

Cheney, J.T. et al., Proterozoic metamorphism of the Tobacco Root Mountains, Montana *in* Brady, J.B., Burger, H.R., Cheney, J.T., and Harms, T.A., eds., 2004, Precambrian Geology of the Tobacco Root Mountains, Montana: Geological Society of America Special Paper 377, p. 105- 129.

Cordua, W.S., 1973, Precambrian geology of the southern Tobacco Root Mountains, Madison County, Montana [Ph.D. thesis]: Bloomington, Indiana University, 248 p.

Dahl, P.S. and Friberg, L.M., 1980, The occurrence and chemistry of epidoteclinozoisites in mafic gneisses from the Ruby Range, southwestern Montana: Contr. To Geology, Univ. Of Wyoming, v. 18, no. 2, p. 77-82.

Dahl, P.S., Holm, D.K., Gardner, E.T., Hubacher, F.A., and Foland, K.A., 1999, New constraints on the timing of Early Proterozoic tectonism in the Black Hills (South Dakota), with implications for docking of the Wyoming province with Laurentia: Geological Society of America Bulletin, v. 111, p. 1335-1349.

Doody, A.E., 2006, Petrology of banded iron formation and phyllite in the Standard Creek contact aureole, southern Gravelly Mountains: 19th Annual Keck Research Symposium in Geology Proceedings, http://keck.wooster.edu/publications.

Erslev, E.A., and Sutter, J.F., 1990, Evidence for Proterozoic mylonization in the northwestern Wyoming province: Geological Society of America Bulletin, v. 102, p. 1681-1694.

Erslev, E.A., 1983, Pre-Beltian geology of the southern Madison Range, southwestern Montana: Montana Bureau of Mines and Geology Memoir 55, 26 p.

Erslev, E.A., 1988, Field guide to pre-beltian geology of the southern Madison and Gravelly Ranges, southwest Montana *in* Lewis and Berg, eds., Montana Bureau of Mines and Geology Special Publication 96, p. 141-149.

Ferry, J.M. and Spear, F.S., 1978, Experimental calibration of the partitioning of Fe and Mg between biotite and garnet. Contributions to Mineralogy and Petrology, v. 66, p. 113-117.

Friberg, N., 1976, Petrology of a metamorphic sequence of upper-amphibolite facies in the central Tobacco Root Mountains, southwestern Montana [Ph.D. thesis]: Bloomington, Indiana University, 146 p.

Giletti, B.J., 1966, Isotopic ages from southwestern Montana: Journal of Geophysical Research, v. 71, p. 4029-4036.

Gillmeister, N.M., 1971, Petrology of Precambrian rocks in the central Tobacco Root Mountains, Madison County, Montana [Ph.D. thesis]: Cambridge, Massachusetts, Harvard University, 210 p.

Gillmeister, N.M., 1972, Cherry Creek Group-Pony Group relationship in the central Tobacco Root Mountains, Madison County, Montana: Northwest Geology, v. 1, p. 21-24.

Hadley, J.B., 1969, Geologic map of the Cameron quadrangle, Madison County, Montana: U.S. Geological Survey Geologic Quadrangle Map GQ-813. Scale 1: 62, 500.

Hanley, T.B., 1975, Structure and petrology of the northwestern Tobacco Root Mountains, Madison County, Montana [Ph.D. thesis]: Bloomington, Indiana University, 289p.

Hanley, T.B., 1976, Stratigraphy and structure of the central fault block, northwestern Tobacco Root Mountains, Madison County, Montana, in Tobacco Root Geological Society, 1976 Field Conference Guidebook: Montana Bureau of Mines and Geology Special Publication 73, p. 7-14.

Harlan, S.S., 1992, Paleomagnetism and Ar/Ar geochronology of selected Proterozoic intrustions, southwest Montana, southeast Wyoming, and central Arizona [Ph.D. dissertation]: University of New Mexico, Albuquerque, 170 p.

Harms, T.A., Brady, J.B., Burger, H.R., Cheney, J.T., 2004, Advances in the geology of the Tobacco Root Mountains, Montana, and their implications for the history of the northern Wyoming province, *in* Brady, J.B., Burger, H.R., Cheney, J.T., and Harms, T.A., eds., 2004, Precambrian Geology of the Tobacco Root Mountains, Montana: Geological Society of America Special Paper 377, p. 227-243.

Hess, D. F., 1967, Geology of pre-Beltian rocks in the central and southern Tobacco Root Mountains with reference to superposed effects of the Laramide-age Tobacco Root batholith [Ph.D. thesis]: Bloomington, Indiana University, 333p.

Hodges, K.V. and Crowley, P.D., 1985, Error estimation and empirical geothermobarometry for pelitic systems. American Mineralogist, v. 70, p. 702-709.

Immega, I.P., and Klein, C., 1976, Mineralogy and petrology of some metamorphic Precambrian iron-formations of southwestern Montana: American Mineralogist, v. 61, p. 1117-1144.

James, H.L., and Weir, K., 1972, Geologic map of the Kelly iron deposit, Sect. 25 T 6S, R 5W., Madison County, Montana: U.S.G.S. open file M.F. 131.

Karasevich, L.P., Garihan, J.M., Dahl, P.S. and Okuma, A.F., 1981, Summary of Precambrian metamorphic and structural history, Ruby Range, Southwest Montana, Montana Geological Society Field Conference Southwest Montana. p. 225-237.

Klein, E.P., 2006, Low grade Precambrian rocks of the central Gravelly Range, SW Montana: 19th Annual Keck Research Symposium in Geology Proceedings, http://keck.wooster.edu/publications.

Labadie, J.E., 2006, New evidence for the Proterozoic Big Sky orogeny recorded in biotite-garnet-sillimanite gneisses from mylonitic zones in the Highland Mountains, Montana.

Millholland, M.A., 1976, Mineralogy and petrology of Precambrian metamorphic rocks of the Gravelly Range, southwestern Montana [M.A. thesis]: Bloomington, Indiana, Indiana University, 135 p.

Mahan, K.H., et al., Dating metamorphic reactions and fluid flow: application to exhumation of high-P granulites in a crustal-scale shear zone, western Canadian Shield, Journal of Metamorphism Geology, 2006, v. 24, p. 193-217.

Matthews, J.A., 2006, Metamorphism of Precambrian rocks in the southern Highland Mountains, southwestern Montana: 19th Annual Keck Research Symposium in Geology Proceedings, http://keck.wooster.edu/publications.

Mogk, D.W., and Henry, D.J., 1988, Metamorphic petrology of the northern Archean Wyoming province, southwestern Montana: Evidence for Archean collisional tectonics, *in* Ernst, W.G., ed., Metamorphism and crustal evolution in the western U.S.: Englewood Cliffs, New Jersey, Prentice-Hall, p. 363-382.

Mogk, D.W., Burger, H.R., Mueller, P.A., D'Arcy, K., Heatherington, A., Wooden, J.L., Abeyta, R.L., Martin, J., Jacob, L.J., 2004, Geochemistry of quartzofeldspathic gneisses and metamorphic mafic rocks of the Indian Creek and Pony-Middle Mountain Metamorphic Suites, Tobacco Root Mountains, Montana, *in* Brady, J.B., Burger, H.R., Cheney, J.T., and Harms, T.A., eds., 2004, Precambrian Geology of the Tobacco Root Mountains, Montana: Geological Society of America Special Paper 377, 256 pp.

Mogk, D.W., Mueller, P.A., and Wooden, J.L., 1992b, The nature of Archean terrane boundaries: An example from the northern Wyoming province: Precambrian Research, v. 55, p. 155-168.

Mogk, D.W., Mueller, P.A., Wooden, J.L., and Bowes, D.R., 1992a, The northern Wyoming province: Contrasts in Archean crustal evolution, in Bartholomew, M.J., et al., eds., Characterization and comparison of ancient and Mesozoic continental margins- Proceedings of the 8th International Conference on Basement Tectonics: Dordrecht, Netherlands, Kluwer Academic Publishers, p. 283-297.

Mueller, P.A., and D'Arcy, K.A., 1990, Sm-Nd systematics of the Late Archean Wyoming Greenstone Terrane: Eos (Transactions, American Geophysical Union), v.71, p. 662.

Mueller, P.A., Heatherington, A., Wooden, J., Mogk, D., and Nutman, A., 1996, Proterozoic evolution of the northwestern Wyoming craton: Geological Society of America Abstracts with Programs, v. 28, no. 7, p. A-314.

Mueller, P.A., Shuster, R.D., Wooden, J.L., Erslev, E.A., and Bowes, D.R., 1993, Age and composition of Archean crystalline rocks from the southern Madison Range, Montana: Geological Society of America Bulletin, v. 105, p. 437-446.

Mueller, P.A., Wooden, J.L., Nutman, A.P., and Mogk, D.W., 1998, Early Archean crust in the northern Wyoming province: Evidence from U-Pb ages of detrital zircons: Precambrian Research, v. 91, p. 295-307.

O'Neill, J.M., 1998, The Great Falls tectonic zone, Montana-Idaho: An Early Proterozoic collisional orogen beneath and south of the Belt Basin, *in* Berg, R.B., ed. Belt Symposium III- 1993: Montana Bureau of Mines and Geology Special Publication 112, p. 222-228.

O'Neill, J.M., Duncan, M.S., and Zartman, R.E., 1988, An Early Proterozoic gneiss dome in the Highland Mountains, southwestern Montana, in Lewis, S.E., and Berg, R.B., eds., Precambrian and Mesozoic plate margins, Montana, Idaho and Wyoming, with field guides for the 8th International Conference on Basement Tectonics: Montana Bureau of Mines and Geology Special Publication 96, p. 81-88.

O'Neill, J.M., and Lopez, D.A., 1985, Character and significance of Great Falls tectonic zone, east-central Idaho and west-central Montana: American Association of Petroleum Geologists Bulletin, v. 69, p. 437-447.

Reid, R.R., 1957, Bedrock geology of the north end of the Tobacco Root Mountains, Madison County, Montana: Montana Bureau of Mines and Geology Memoir 36, 25p.

Reid, R.R., 1963, Metamorphic rocks of the northern Tobacco Root Mountains, Madison County: Geological Society of America Bulletin, v. 74, p. 293-306.

Root, F.K., 1965, Structure, petrology, and mineralogy of pre-Beltian metamorphic rocks of the Pony-Sappington area, Madison County, Montana [Ph.D. thesis]: Bloomington, Indiana University, 184 p.

Schwab, A.R., Shearing in the mylonites of the McAtee Bridge Ridge, Montana, USA: compressional shearing in the Big Sky orogeny: 19th Annual Keck Research Symposium in Geology Proceedings, http://keck.wooster.edu/publications.

Spear, F.S. and Kohn, M.J., 2001, Program GTB: GeoThermoBarometry. Rensselaer Polytechnic Institute. 30 March 2006, http://ees2.geo.rpi.edu/MetaPetaRen/GTB_Prog/GTB.html

Spear, Frank S., 1993, Metamorphic Phase Equilibria and Pressure-Temperature-Time Paths, Mineralogical Society of America Monograph, 344 p.

Tansley, W., Schafer, P.A., and Hart, L.H., 1933, A geological reconnaissance of the Tobacco Root Mountains, Madison County, Montana: Montana Bureau of Mines and Geology Memoir 9, 57p.

Vargo, A.G., 1990, Structure and petrography of the pre-beltian rocks of the north-central Gravelly Range, Montana [M. S. thesis]: Fort Collins, Colorado State University.

Vitaliano, C.J., Burger, H.R., Cordua, W.S., Hanley, T.B., Hess, D.F., and Root, F.K., 1979a, Geologic map of southern Tobacco Root Mountains, Madison County, Montana: Geological Society of America Map and Chart Series MC31, scale 1:62,500, 1 sheet, 8 p. text.

Vitaliano, C.J., Burger, H.R., Cordua, W.S., Hanley, T.B., Hess, D.F., and Root, F.K., 1979b, Explanatory text to accompany geologic map of the southern Tobacco Root Mountains, Madison County, Montana: Geological Society of America Map and Chart Series MC31, scale 1:62,500, 1 sheet, 8 p. text.

Williams, M.L., Jercinovic, M.J., Goncalves, P., Mahan, K., 2006, Format and philosophy for collecting, compiling, and reporting microprobe monazite ages. Chemical Geology, v. 225, p. 1-15.

Wilson, Michael L., 1981, Origin of Archean lithologies in the southern Tobacco Root and Northern Ruby Ranges of southwestern Montana: Montana Geological Society Field Conference Southwest Montana, p. 37-43.
Website: Monazite Research at UMass, Monazite Techniques. Viewed 04/19/06. http://www.geo.umass.edu/probe/Monazite%20techniques-summary%20frames.htm.

APPENDICES

Appendix a

SEM analyses used for GTB analysis of sample DG-2a
SEM analyses used for GTB analysis of sample DG-35b

Appendix b

Table of analyses of monazites from sample DG-29 and ages given
Table of analyses of monazites from sample DG-8a and ages given

2a Thermobarometry analyses

Garnet 1 All pressures used plag 1- plag 2 was funky

Garnet3

Elmt	Atomic %		Compound %	Nos. of ions	P6	
Na	0.213	Na2O	0.281	0.043		
Mg	3.663	MgO	6.281	0.732		
Al	10.069	Al2O3	21.836	2.013		
Si	15.106	SiO2	38.612	3.020		
Ca	0.410	CaO	0.979	0.082		
Ti	0.033	TiO2	0.113	0.007		
Mn	0.096	MnO	0.291	0.019		
Fe	10.376	FeO	31.712	2.074		
O	60.034		100.104	12.000	Mg/(Mg+Fe)=	0.26
				7.989		

Biotite3

Elmt	Atomic %		Compound %	Nos. of ions	T1
Na	0.289	Na2O	0.396	0.054	plots out of bounds
Mg	10.710	MgO	19.067	2.009	
Al	8.110	Al2O3	18.260	1.521	
Si	14.942	SiO2	39.648	2.803	
K	4.077	K2O	8.482	0.765	
Ca	0.093	CaO	0.231	0.018	
Ti	0.470	TiO2	1.659	0.088	
Mn	-0.019	MnO	-0.061	-0.004	
Fe	2.685	FeO	8.520	0.504	
O	58.642		96.202	11.000	
				7.758	Mg/(Mg+Fe)= 0.8

Garnet 2

Garnet2_rim

Elmt	Atomic %		Compound %	Nos. of ions	P7	
Na	0.321	Na2O	0.419	0.064		
Mg	4.697	MgO	7.983	0.941		
Al	10.019	Al2O3	21.535	2.007		
Si	14.974	SiO2	37.935	2.999		
Ca	0.424	CaO	1.002	0.085		
Ti	-0.005	TiO2	-0.015	-0.001		
Mn	0.136	MnO	0.408	0.027		
Fe	9.524	FeO	28.850	1.908		
O	59.909		98.117	12.000	Mg/(Mg+Fe)=	0.33

Biotite2_1

Elmt	Atomic %		Compound %	Nos. of ions	T2

Na	0.441	Na2O	0.607	0.083	
Mg	9.910	MgO	17.714	1.859	
Al	8.472	Al2O3	19.151	1.589	
Si	14.707	SiO2	39.185	2.758	
K	4.130	K2O	8.626	0.775	
Ca	0.031	CaO	0.078	0.006	
Ti	0.637	TiO2	2.257	0.119	
Mn	-0.023	MnO	-0.073	-0.004	
Fe	3.048	FeO	9.711	0.572	
O	58.647		97.256	11.000	Mg/(Mg+Fe)= 0.76

Biotite2_3

Elmt	Atomic %		Compound %	Nos. of ions	T3
Na	0.488	Na2O	0.662	0.092	
Mg	9.603	MgO	16.933	1.815	
Al	9.673	Al2O3	21.571	1.828	
Si	13.862	SiO2	36.433	2.620	
K	4.814	K2O	9.919	0.910	
Ca	0.033	CaO	0.080	0.006	
Ti	0.346	TiO2	1.208	0.065	
Mn	0.011	MnO	0.036	0.002	
Fe	2.974	FeO	9.348	0.562	
O	58.196		96.190	11.000	Mg/(Mg+Fe)= 0.76

Garnet2_3

Elmt	Atomic %		Compound %	Nos. of ions	P8
Na	0.216	Na2O	0.284	0.043	
Mg	3.672	MgO	6.296	0.735	
Al	10.122	Al2O3	21.950	2.027	
Si	14.915	SiO2	38.119	2.986	
Ca	0.425	CaO	1.014	0.085	
Mn	0.144	MnO	0.433	0.029	
Fe	10.572	FeO	32.309	2.117	
O	59.934		100.405	12.000	Mg/(Mg+Fe)= 0.258

Garnet 3

Garnet3_rim P9

Elmt	Atomic %		Compound %	Nos. of ions
Na	0.252	Na2O	0.324	0.051
Mg	3.851	MgO	6.444	0.772
Al	9.958	Al2O3	21.073	1.996
Si	14.891	SiO2	37.137	2.985
Ca	0.410	CaO	0.955	0.082
Ti	-0.007	TiO2	-0.023	-0.001
Mn	0.172	MnO	0.506	0.034
Fe	10.604	FeO	31.624	2.126

O	59.868		98.040	12.000	Mg/(Mg+Fe)=	0.27
Biotite3_1						
Elmt	Atomic %		Compound %	Nos. of ions	T4	
Na	0.307	Na2O	0.407	0.058		
Mg	10.134	MgO	17.465	1.908		
Al	9.024	Al2O3	19.669	1.699		
Si	14.489	SiO2	37.219	2.728		
K	4.467	K2O	8.996	0.841		
Ca	0.027	CaO	0.064	0.005		
Ti	0.216	TiO2	0.739	0.041		
Mn	-0.005	MnO	-0.015	-0.001		
Fe	2.926	FeO	8.989	0.551		
O	58.415		93.531	11.000	Mg/(Mg+Fe)=	0.78
Garnet 3_2 analysis 4 bc- -2.666						
Elmt	Atomic %		Compound %	Nos. of ions	P10	
Na	0.299	Na2O	0.407	0.060		
Mg	4.982	MgO	8.812	0.997		
Al	10.204	Al2O3	22.826	2.041		
Si	15.016	SiO2	39.589	3.004		
Ca	0.413	CaO	1.017	0.083		
Ti	0.009	TiO2	0.033	0.002		
Mn	0.114	MnO	0.354	0.023		
Fe	8.974	FeO	28.290	1.795		
O	59.989		101.327	12.000	Mg/(Mg+Fe)=	0.36
				8.004		
Biotite3_2						
Elmt	Atomic %		Compound %	Nos. of ions	T5	
Na	0.363	Na2O	0.478	0.068		
Mg	10.148	MgO	17.369	1.908		
Al	8.499	Al2O3	18.397	1.598		
Si	14.600	SiO2	37.244	2.745		
K	4.184	K2O	8.366	0.787		
Ca	0.140	CaO	0.332	0.026		
Ti	0.434	TiO2	1.471	0.082		
Mn	0.039	MnO	0.116	0.007		
Fe	3.089	FeO	9.422	0.581		
O	58.505		93.195	11.000	Mg/(Mg+Fe)=	0.77

Text File Used for Spear and Kohn's Program Geothermobarometry for sample DG-2a

15

Sample	Point	Wt%tot	Xpos	Ypos	CSi	CAl	CTi
Garnet1_core	1	98.76	0	0	2.972	2.033	0
Garnet2_rim	2	99.14	0	0	2.998	2.035	0.003
Garnet3	3	100.1	0	0	3.02	2.013	0.007
Biotite3	4	96.2	0	0	2.803	1.521	0.088
Plag1	5	100.22	0	0	2.751	1.254	0
Sillimanite1	6	100.08	0	0	0.979	2.029	0
Plag2	7	98.75	0	0	2.796	1.207	0
Garnet4	8	99.47	0	0	2.999	2.026	0
Biotite4	9	97.57	0	0	2.803	1.605	0.048
Garnet2_core	10	99.34	0	0	3	2.01	0
Garnet2_rim	11	98.12	0	0	2.999	2.007	0
Biotite2_1	12	97.26	0	0	2.758	1.589	0.119
Garnet2_2	13	101.87	0	0	3.025	2.02	0
Biotite2_2	14	96.14	0	0	2.738	1.581	0.147
Biotite2_3	15	96.19	0	0	2.62	1.828	0.065
Garnet2_3	16	100.41	0	0	2.986	2.027	0
Garnet3_core	17	100.15	0	0	2.981	2.018	0
Garnet3_rim	18	98.04	0	0	2.985	1.996	0
Biotite3_1	19	93.53	0	0	2.728	1.699	0.041
Garnet3_2	20	101.327	0	0	3.004	2.041	0.002
Biotite3_2	21	93.2	0	0	2.745	1.598	0.082
Biotite 3_4	22	96.456	0	0	2.741	1.561	0.164
Garnet 3_4	23	100.659	0	0	2.985	2.009	0
Garnet 3_4end	24	100.659	0	0	2.985	2.009	0

Sample	CFe3+	CMg	CFe2+	CMn	CCa	CNa	CK
Garnet1_core	0	1.21	1.687	0.012	0.075	0.05	0
Garnet2_rim	0	0.947	1.883	0.02	0.085	0.06	0
Garnet3	0	0.732	2.074	0.019	0.082	0.043	0
Biotite3	0	2.009	0.504	0	0.018	0.054	0.765
Plag1	0	0	0	0	0.232	0.767	0.004
Sillimanite1	0	0	0	0	0	0	0
Plag2	0	0	0	0	0.172	0.848	0.003
Garnet4	0	1.112	1.736	0.016	0.073	0.06	0
Biotite4	0	2.217	0.295	0	0	0	0.761
Garnet2_core	0	1.175	1.685	0.012	0.093	0.037	0
Garnet2_rim	0	0.941	1.908	0.027	0.085	0.064	0
Biotite2_1	0	1.859	0.572	0	0.006	0.083	0.775
Garnet2_2	0	0.954	1.84	0.013	0.084	0.059	0
Biotite2_2	0	1.941	0.496	0	0	0.086	0.777
Biotite2_3	0	1.815	0.562	0.002	0.006	0.092	0.91
Garnet2_3	0	0.735	2.117	0.029	0.085	0.043	0
Garnet3_core	0	1.228	1.668	0.008	0.085	0.046	0
Garnet3_rim	0	0.772	2.126	0.034	0.082	0.051	0
Biotite3_1	0	1.908	0.551	0	0.005	0.058	0.841
Garnet3_2	0	0.997	1.795	0.023	0.083	0.06	0
Biotite3_2	0	1.908	0.581	0.007	0.026	0.068	0.787
Biotite 3_4	0	1.961	0.444	0	0.012	0.128	0.738
Garnet 3_4	0	1.091	1.81	0.014	0.083	0.042	0
Garnet 3_4end	0	1.091	1.81	0.014	0.083	0.042	0

35b Thermobarometry analyses

Plot number on Graph

Analyses without corrections for Fe3+, since correcting for Fe 3+ caused reactions to plot out of bounds

From Garnet 1

Garnet 5 and Biotite 5

T1 about 710

Biotite1_5
Garnet 1 Biotite 5 next to plag

Elmt Type	Spect.	Element %	Atomic %	Compound	Compound %	Nos. of ions
Mg K	ED	6.94	6.79	MgO	11.50	1.27
Al K	ED	9.99	8.81	Al2O3	18.88	1.65
Si K	ED	16.95	14.36	SiO2	36.27	2.69
K K	ED	8.33	5.07	K2O	10.04	0.95
Ca K	ED	0.04*	0.02*	CaO	0.05*	0.00*
Ti K	ED	2.28	1.13	TiO2	3.81	0.21
Fe K	ED	12.05	5.13	FeO	15.50	0.96
O		39.47	58.68			11.00
Total		96.05	100.00		96.05	

Cation sum 7.74

Mg/Mg+Fe= 0.56950673

Garnet1_5
Garnet 1 analysis 5

P6-calculated using plag2 about 5.8 kb

Elmt Type	Spect.	Element %	Atomic %	Compound	Compound %	Nos. of ions
Mg K	ED	3.51	3.45	MgO	5.83	0.69
Al K	ED	11.78	10.41	Al2O3	22.26	2.08
Si K	ED	17.84	15.15	SiO2	38.17	3.02
Ca K	ED	0.77	0.46	CaO	1.07	0.09
Ti K	ED	0.04*	0.02*	TiO2	0.06*	0.00*
Fe K	ED	24.23	10.34	FeO	31.17	2.06
O		40.39	60.18			12.00
Total		98.56	100.00		98.56	

Cation sum 7.94

Mg/Mg+Fe= 0.25090909

Garnet core and biotite 3

didn't use these- garnet failed stoichio- metry test

Garnet1_1

Elmt Type	Spect.	Element %	Atomic %	Compound	Compound %	Nos. of ions
Mg K	ED	3.46	3.39	MgO	5.74	0.68
Al K	ED	11.48	10.14	Al2O3	21.69	2.02
Si K	ED	17.83	15.13	SiO2	38.14	3.02
Ca K	ED	0.74	0.44	CaO	1.04	0.09
Mn K	ED	1.18	0.51	MnO	1.52	0.10
Fe K	ED	24.12	10.29	FeO	31.03	2.06
O		40.35	60.10			12.00

Total		99.17	100.00		99.17		Mg/Mg+Fe= 0.24817518
			Cation sum	7.97			

Biotite3

Elmt Type	Spect.	Element %	Atomic %	Compound	Compound %	Nos. of ions
Mg K	ED	7.57	7.49	MgO	12.55	1.40
Al K	ED	9.96	8.88	Al2O3	18.82	1.66
Si K	ED	16.80	14.39	SiO2	35.93	2.69
K K	ED	7.03	4.33	K2O	8.47	0.81
Ca K	ED	0.11	0.07	CaO	0.16	0.01
Ti K	ED	2.30	1.16	TiO2	3.84	0.22
Mn K	ED	-0.02*	-0.01*	MnO	-0.03*	0.00*
Fe K	ED	11.12	4.79	FeO	14.30	0.89
O		39.18	58.91			11.00
Total		94.05	100.00		94.05		Mg/Mg+Fe= 0.61135371
			Cation sum	7.67			

Points from Garnet 2

Biotite2_2 — T2 about 480

Elmt Type	Spect.	Element %	Atomic %	Compound	Compound %	Nos. of ions
Na K	ED	0.33	0.36	Na2O	0.45	0.07
Mg K	ED	7.00	7.05	MgO	11.60	1.33
Al K	ED	9.74	8.84	Al2O3	18.40	1.66
Si K	ED	16.32	14.23	SiO2	34.91	2.68
K K	ED	7.95	4.98	K2O	9.57	0.94
Ca K	ED	0.01*	0.00*	CaO	0.01*	0.00*
Ti K	ED	1.96	1.00	TiO2	3.28	0.19
Fe K	ED	11.54	5.06	FeO	14.85	0.95
O		38.22	58.49			11.00
Total		93.07	100.00		93.07	
			Cation sum	7.81			Mg/Mg+Fe= 0.58333333

Garnet2_2 (analysis 3 on picture) — P7 with plag 5 about 1.8Kb

Elmt Type	Spect.	Element %	Atomic %	Compound	Compound %	Nos. of ions

Mg K	ED	2.53	2.49	MgO	4.20	0.50
Al K	ED	11.61	10.27	Al2O3	21.94	2.05
Si K	ED	17.79	15.12	SiO2	38.07	3.02
Ca K	ED	0.71	0.43	CaO	1.00	0.08
Mn K	ED	1.43	0.62	MnO	1.84	0.12
Fe K	ED	25.62	10.95	FeO	32.96	2.19
O		40.31	60.13			12.00
Total		100.01	100.00		100.01	
			Cation sum	7.96		

Mg/Mg+Fe= 0.18587361

Points from Garnet 3

Garnet3_1

Elmt Type	Spect.	Element %	Atomic %	Compound	%	Nos. of ions
Na K	ED	0.26	0.27	Na2O	0.35	0.05
Mg K	ED	2.86	2.80	MgO	4.74	0.56
Al K	ED	11.49	10.13	Al2O3	21.71	2.03
Si K	ED	17.66	14.95	SiO2	37.77	2.99
Ca K	ED	0.76	0.45	CaO	1.07	0.09
Mn K	ED	1.30	0.56	MnO	1.68	0.11
Fe K	ED	25.57	10.89	FeO	32.89	2.18
O		40.31	59.94			12.00
Total		100.21	100.00		100.21	
			Cation sum	8.02		

P8 with plag 5

Mg/Mg+Fe= 0.20437956

Biotite3_1

Elmt Type	Spect.	Element %	Atomic %	Compound	%	Nos. of ions
Mg K	ED	7.39	7.04	MgO	12.25	1.32
Al K	ED	10.24	8.79	Al2O3	19.34	1.65
Si K	ED	17.45	14.40	SiO2	37.33	2.70
K K	ED	8.32	4.93	K2O	10.03	0.92
Ca K	ED	0.04*	0.02*	CaO	0.06*	0.00*
Ti K	ED	2.27	1.10	TiO2	3.78	0.21
Fe K	ED	12.05	5.00	FeO	15.51	0.94
O		40.53	58.71			11.00
Total		98.29	100.00		98.29	
			Cation sum	7.74		

T3

Mg/Mg+Fe= 0.5840708

Garnet3_2

P9 with plag 5

Elmt	Spect.	Element	Atomic	Compound	Nos. of

Type		%	%		%	ions
Na K	ED	0.16	0.17	Na2O	0.21	0.03
Mg K	ED	2.67	2.67	MgO	4.42	0.53
Al K	ED	11.26	10.14	Al2O3	21.27	2.03
Si K	ED	17.21	14.90	SiO2	36.82	2.98
Ca K	ED	0.69	0.42	CaO	0.96	0.08
Mn K	ED	1.58	0.70	MnO	2.04	0.14
Fe K	ED	25.40	11.06	FeO	32.68	2.21
O		39.44	59.94			12.00
Total		98.40	100.00			98.40

Cation sum 8.02

Mg/Mg+Fe= 0.19343066

biotite3_2

T4

Elmt Type	Spect.	Element %	Atomic %		Compound %	Nos. of ions
Mg K	ED	6.55	6.57	MgO	10.85	1.23
Al K	ED	9.49	8.57	Al2O3	17.93	1.61
Si K	ED	16.68	14.48	SiO2	35.69	2.71
K K	ED	8.05	5.02	K2O	9.70	0.94
Ca K	ED	0.09*	0.06*	CaO	0.13*	0.01*
Ti K	ED	2.28	1.16	TiO2	3.81	0.22
Fe K	ED	12.42	5.42	FeO	15.98	1.02
O		38.52	58.71			11.00
Total		94.08	100.00		94.08	

Cation sum 7.74

Mg/Mg+Fe= 0.54666667

Garnet 4 analyses

Biotite4_1

T5

Elmt Type	Spect.	Element %	Atomic %		Compound %	Nos. of ions
Mg K	ED	7.78	7.60	MgO	12.91	1.43
Al K	ED	9.99	8.78	Al2O3	18.87	1.65
Si K	ED	16.94	14.31	SiO2	36.23	2.68
K K	ED	8.16	4.95	K2O	9.82	0.93
Ca K	ED	0.05*	0.03*	CaO	0.08*	0.01*
Ti K	ED	2.11	1.05	TiO2	3.52	0.20
Fe K	ED	10.93	4.65	FeO	14.07	0.87

O		39.53	58.64		11.00	
Total		95.49	100.00	95.49		
			Cation sum	7.76		Mg/Mg+Fe= 0.62173913

Garnet4_1 P10 with plag 5

Elmt Type	Spect.	Element %	Atomic %		Compound %	Nos. of ions
Mg K	ED	2.42	2.42	MgO	4.01	0.48
Al K	ED	11.28	10.19	Al2O3	21.32	2.04
Si K	ED	17.22	14.93	SiO2	36.84	2.99
Ca K	ED	0.89	0.54	CaO	1.24	0.11
Mn K	ED	1.83	0.81	MnO	2.36	0.16
Fe K	ED	25.44	11.09	FeO	32.73	2.22
O		39.42	60.01			12.00
Total		98.50	100.00		98.50	
			Cation sum		8.00	Mg/Mg+Fe= 0.17777778

Text File used for Spear and Kohn's Program Geothermobarometry for sample DG-35b

15

Sample	Point	Wt%tot	Xpos	Ypos	CSi	CAl	CTi	CFe3+
Garnet1_1	1	99.17	0	0	3.02	2.02	0	0
Garnet1_rim	2	99.56	0	0	3	2.02	0	0
Garnet1_3	3	100.12	0	0	2.98	2.03	0	0
Garnet1_4	4	99.34	0	0	3	2.05	0	0
AlSi1	5	100.76	0	0	0.96	2.04	0	0
Biotite1	6	96.08	0	0	2.69	1.66	0.21	0
Biotite2	7	96.7	0	0	2.69	1.66	0.22	0
Biotite3	8	94.05	0	0	2.69	1.66	0.22	0
Plag1	9	101.81	0	0	2.74	1.26	0	0
Plag2	10	101.25	0	0	2.73	1.28	0	0
Garnet1_5	11	98.56	0	0	3.02	2.08	0	0
Biotite1_5	12	96.05	0	0	2.69	1.65	0.21	0
Plag3	13	101.81	0	0	2.73	1.28	0	0
Garnet2_core	14	99.7	0	0	2.99	2.03	0	0
Garnet2_1	15	98.93	0	0	3	2.04	0	0
Plag4	16	100.76	0	0	2.73	1.28	0	0
Biotite2_1	17	94.12	0	0	2.69	1.64	0.22	0
Biotite2_2	18	93.07	0	0	2.68	1.66	0.19	0
Garnet2_2	20	100.01	0	0	3.02	2.05	0	0
Plag5	21	99.92	0	0	2.73	1.28	0	0
Garnet2_core	22	98.38	0	0	2.98	2.07	0	0
Garnet2_5	23	100.72	0	0	3.03	2.04	0	0
Biotite2_5	24	95.24	0	0	2.7	1.67	0.21	0
Garnet3_1	25	100.21	0	0	2.99	2.03	0	0
Biotite3_1	26	98.29	0	0	2.7	1.65	0.21	0
Garnet3_2	27	98.4	0	0	2.98	2.03	0	0
Biotite3_2	28	94.08	0	0	2.71	1.61	0.22	0
Garnet4_1	29	98.5	0	0	2.99	2.04	0	0
Biotite4_1	30	95.49	0	0	2.68	1.65	0.2	0

Text File used for Spear and Kohn's Program Geothermobarometry for sample DG-35b

Sample	CMg	CFe2+	CMn	CCa	CNa	CK
Garnet1_1	0.68	0	0.1	0.09	0	0
Garnet1_rim	0.74	2.01	0.1	0.11	0	0
Garnet1_3	0.74	2.04	0.1	0.11	0	0
Garnet1_4	0.75	2	0.08	0.1	0	0
AlSi1	0	0.01	0	0	0	0
Biotite1	1.33	0.91	0	0	0	0.92
Biotite2	1.29	0.91	0.01	0.01	0	0.95
Biotite3	1.4	0.89	0	0.01	0	0.81
Plag1	0	0	0	0.24	0.74	0
Plag2	0	0	0	0.25	0.73	0.01
Garnet1_5	0.69	2.06	0	0.09	0	0
Biotite1_5	1.27	0.96	0	0	0	0.95
Plag3	0	0	0	0.25	0.73	0
Garnet2_core	0.68	2.09	0.1	0.1	0	0
Garnet2_1	0.6	2.11	0.14	0.08	0	0
Plag4	0	0	0	0.25	0.74	0
Biotite2_1	1.23	1.01	0	0.01	0	0.95
Biotite2_2	1.33	0.95	0	0	0.07	0.94
Garnet2_2	0.5	2.19	0.12	0.08	0	0
Plag5	0	0	0	0.26	0.74	0
Garnet2_core	0.55	2.16	0.13	0.1	0	0
Garnet2_5	0.44	2.2	0.15	0.09	0	0
Biotite2_5	1.26	0.96	0	0	0	0.91
Garnet3_1	0.56	2.18	0.11	0.09	0.05	0
Biotite3_1	1.32	0.94	0	0	0	0.92
Garnet3_2	0.53	2.21	0.14	0.08	0.03	0
Biotite3_2	1.23	1.02	0	0.01	0	0.94
Garnet4_1	0.48	2.22	0.16	0.11	0	0
Biotite4_1	1.43	0.87	0	0.01	0	0.93

Microprobe Analysis of Sample DG-8a: Monazite Ages

M1 core

Pt	Y ppm	Pb ppm	U ppm	age	comments
1	5054	4329	2039	1800	
2	4533	4373	2148	1799	
3	4398	4348	2002	1826	
4	4549	4361	2196	1798	
5	4617	4288	1987	1802	
6	4445	4378	2154	1800	
7	4525	4404	2040	1830	
8	4415	4483	2193	1812	
9	4544	4387	2002	1844	
9	4564	4372	2084	1812	Average
9	197	54	87	17	Standard deviation of the measurements
9	66	18	29	6	Standard deviation of the mean or standard error

M2 core (in red because of the very large standard deviation)

Pt	Y	Pb	U	age	comments
1	23171	5570	7923	1721	
2	23311	5197	6713	1676	
3	24526	5020	4073	1862	
4	24541	5090	4177	1854	
5	22088	5348	8618	1623	
6	22085	5602	8311	1677	
6	23287	5304	6635	1735	Average
6	1096	245	2050	100	Standard deviation of the measurements
6	447	100	837	41	Standard deviation of the mean or standard error

M2 rim

Pt	Y	Pb	U	age	comments
1	4765	4734	1929	1826	
2	4568	4711	1951	1802	
3	5038	4666	1877	1851	
4	4548	4722	1940	1804	
5	5274	4841	1654	1856	
6	5121	4588	1837	1735	
6	4885	4710	1864	1812	Average
6	303	83	112	44	Standard deviation of the measurements
6	124	34	46	18	Standard deviation of the mean or standard error

Statistical Analysis of all data	
Mean	1810.759
Standard Error	5.08536
Median	1825.5
Mode	1804
Standard Deviation	37.36961
Sample Variance	1396.488
Kurtosis	0.325784
Skewness	-1.12988
Range	137
Minimum	1719
Maximum	1856
Sum	97781
Count	54
Confidence Level(95.0%)	10.19994

Statistical Analysis of all data except M2 core and M6 core	
Mean	1819.667
Standard Error	4.057688
Median	1827.5
Mode	1804
Standard Deviation	28.11249
Sample Variance	790.3121
Kurtosis	1.975678
Skewness	-1.3676
Range	121
Minimum	1735
Maximum	1856
Sum	87344
Count	48
Confidence Level(95.0%)	8.163016

M3 core

Pt	Y ppm	Pb ppm	U ppm	age	comments
1	24067	4544	3583	1836	
2	24857	4573	3080	1829	
3	25097	4382	2809	1833	
4	25806	4430	2944	1828	
5	15194	3810	2024	1852	
6	24818	4568	3623	1790	
7	25843	4390	2470	1854	
8	24098	4500	2634	1830	
8	23722	4399	2895	1831	Average
8	3509	250	542	20	Standard deviation of the measurements
8	1241	88	192	7	Standard deviation of the mean or standard error

M3 rim

Pt	Y	Pb	U	age	comments
1	2010	5003	615	1763	
2	1972	4928	625	1754	
3	2185	4342	584	1643	
4	1957	4732	889	1840	
5	2101	4565	793	1804	
6	2180	4795	653	1845	
7	854	4670	584	1739	
8	2126	4769	771	1847	
8	1923	4725	689	1779	Average
8	441	207	114	70	Standard deviation of the measurements
8	156	73	40	25	Standard deviation of the mean or standard error

M4 core

Pt	Y	Pb	U	age	comments
1	26739	3407	5119	1821	
2	25498	4042	4173	1833	
3	24653	4382	3655	1837	
4	24817	4510	3879	1811	
5	25365	4034	3445	1834	
5	25414	4075	4054	1827	Average
5	822	428	654	11	Standard deviation of the measurements
5	368	191	292	5	Standard deviation of the mean or standard error

Statistical Analysis of M2 core and M6 core data only

Mean	1737.5
Standard Error	19.94595
Median	1726
Mode	#N/A
Standard Deviation	69.0948
Sample Variance	4774.091
Kurtosis	0.307551
Skewness	0.537443
Range	239
Minimum	1623
Maximum	1862
Sum	20850
Count	12
Confidence Level(95.0%)	43.90074

M4 rim

Pt	Y ppm	Pb ppm	U ppm	age	comments
1	2220	4814	892	1806	
2	2351	4893	904	1846	
3	2268	4918	952	1820	
4	2353	4814	826	1853	
5	2164	4837	959	1804	
6	2844	4627	1143	1838	
7	2258	4740	988	1844	
7	2351	4806	952	1830	Average
7	228	98	100	20	Standard deviation of the measurements
7	86	37	38	8	Standard deviation of the mean or standard error

M5 core

Pt	Y	Pb	U	age	comments
1	738	4133	1567	1825	
2	980	3915	2026	1829	
3	1008	3894	2023	1827	
4	972	3983	2012	1824	
5	1003	3890	1967	1834	
6	928	3803	2005	1829	
6	938	3936	1933	1828	Average
6	102	112	181	4	Standard deviation of the measurements
6	42	46	74	2	Standard deviation of the mean or standard error

M6 core

Pt	Y	Pb	U	age	comments
1	1104	5562	539	1719	
2	1132	5864	627	1728	
3	1273	5721	665	1748	
4	1262	5936	756	1781	
5	1262	5636	693	1724	
6	1028	5576	596	1737	
6	1176	5715	646	1739	Average
6	103	155	76	23	Standard deviation of the measurements
6	42	63	31	9	Standard deviation of the mean or standard error

Microprobe Analysis of Sample DG-29: Monazite Ages

M1

Pt	Y ppm	Pb ppm	U ppm	age	comments
1	11589	5164	2501	2583	
2	12448	4823	2663	2658	
3	11755	4697	2439	2625	
4	12604	4674	2745	2610	
5	12424	5174	2988	2571	
5	12164	4906	2667	2609	Average
5	458	246	217	35	Standard deviation of the measurements
5	205	110	97	16	Standard deviation of the mean or standard error

M3

Pt	Y	Pb	U	age	comments
1	16595	6332	2826	2568	
2	16453	4192	1591	2525	
3	14638	6373	3564	2581	
4	14609	5218	2588	2521	
5	15837	4894	2458	2518	
6	17038	3598	1291	2477	
6	15861	5101	2386	2531	Average
6	1033	1120	832	38	Standard deviation of the measurements
6	422	457	340	16	Standard deviation of the mean or standard error

M4

Pt	Y	Pb	U	age	comments
1	12279	3908	2510	2627	
2	12625	4661	3049	2557	
3	15941	9049	5841	2602	
4	15950	9955	6914	2524	
5	15923	10032	6683	2550	
6	11324	5180	2939	2572	
7	12274	5572	3601	2604	
8	11491	4168	2151	2554	
8	13475	6565	4211	2573	Average
8	2083	2646	1948	34	Standard deviation of the measurements
8	736	936	689	12	Standard deviation of the mean or standard error

Statistical Analysis of all data

Mean	2569.842105
Standard Error	10.37548369
Median	2571
Mode	#N/A
Standard Deviation	45.22568488
Sample Variance	2045.362573
Kurtosis	-0.209503142
Skewness	-0.050535864
Range	181
Minimum	2477
Maximum	2658
Sum	48827
Count	19